Development of a void ratio-moisture ratio-net stress framework for the prediction of the volumetric behavior of unsaturated granular materials

Yaghoubi, Ehsan, Disfani, Mahdi, Arulrajah, Arul and Kodikara, J (2019) Development of a void ratio-moisture ratio-net stress framework for the prediction of the volumetric behavior of unsaturated granular materials. Soils and Foundations. ISSN 0038-0806

Development of a Void Ratio-Moisture Ratio-Net Stress Framework for Prediction of the Volumetric Behavior of Unsaturated Granular Materials

Ehsan Yaghoubi
Coffey, A Tetra Tech Company, Melbourne, Australia.
E-mail: ehsan.yaghoubi@coffey.com

Mahdi M. Disfani*
Department of Infrastructure Engineering, The University of Melbourne, Melbourne, Australia.
E-mail: mahdi.miri@unimelb.edu.au

Arul Arulrajah
Department of Civil and Construction Engineering, Swinburne University of Technology, Melbourne, Australia.
E-mail: aarulrajah@swin.edu.au

Jayantha Kodikara
Department of Civil Engineering, Monash University, Melbourne, Australia.
E-mail: jayantha.kodikara@monash.edu

* Corresponding Author:

Dr. Mahdi M DISFANI
Department of Infrastructure Engineering, Melbourne School of Engineering
The University of Melbourne, Parkville, VIC 3010, Australia
Email: mahdi.miri@unimelb.edu.au
Phone: + 61 3 8344 5972

Abstract

Despite extensive research on the behavior of unsaturated fine-grained materials, there is still a lack of understanding of the volumetric behavior of unsaturated granular materials. In this research, a model has been developed to predict the fundamental volumetric behavior of unsaturated granular materials through loading and wetting state paths. In this regard, a loading-wetting surface was developed in a space of void ratio-moisture ratio-net stress. A distinctive feature of the proposed model is the relative simplicity in obtaining the model parameters using conventional geotechnical testing equipment. Two types of recycled granular materials commonly used in unbound pavements were used, namely recycled crushed brick (CB) and excavation waste rock (WR). The uniqueness of the developed surface was evaluated by applying a number of loading and wetting state paths. Results indicate that the developed surface is unique in loading state paths; however, it only shows uniqueness to wetting for stress levels greater than 2000 kPa. The proposed model seeks to introduce the application of unsaturated soil mechanics theory for predicting the behavior of granular materials in the field, by providing a practical and cost effective methodology.

Keywords: unsaturated granular material; recycled materials; volumetric behavior; constitutive surface; compaction.

1 Introduction

Industrial activities in the modern world have led to an increase in the amounts of solid waste generated, hence the urgent need for development of effective waste management strategies. Construction and demolition (C&D) activities are a major source of solid wastes. Crushed brick (CB) and waste rock (WR) form a major source of C&D materials. CB is generated through the demolition of structures, mainly masonry buildings, but it may include proportions of other materials such as concrete, concrete mortar, and crushed glass. WR is produced during excavations carried out with purposes such as site preparation for infrastructure construction and mining (Arulrajah et al. 2013). Studies of Wu et al. (2009), Cameron et al. (2012), Arulrajah et al. (2013), Azam and Cameron (2013), Arulrajah et al. (2014), and Suddeepong et al. (2018) show that CB and WR have mechanical properties comparable to typical quarry materials. Generally, since civil engineering infrastructures such as pavements and embankments require a significant amount of materials, utilization of C&D materials could be both economically and environmentally beneficial due to minimization of the demand for the precious natural resources and landfill space (Suksiripattanapong et al., 2017). Geoenvironmental assessment of CB and WR by determination of total and leachate concentration of the contaminants has shown that these materials can safely be used in pavements and embankment fills (Arulrajah et al., 2013; Rahman et al., 2014).

Granular recycled materials used in the construction of embankments or pavements are unsaturated for the majority of their service life. However, fewer studies have been conducted to develop unsaturated constitutive models for these materials since the influence of suction is normally considered only for fine-grained materials. Nevertheless, results of studies by Ba et al. (2013), Azam and Cameron (2013), and Yaghoubi et al. (2016), have demonstrated the effect of suction on the mechanical characteristics of granular materials. Cary and Zapata (2011) and Azam et al.

(2013) have improved the existing predictive resilient modulus models by incorporating a suction-related term indicating that suction, despite being low, influences the behavior of unsaturated granular materials. Mitigating uncertainties by developing constitutive models for predicting the volumetric behavior of recycled granular materials is necessary for widespread application of C&D materials in construction industries.

1.1 Current Volume Change Constitutive Models

Constitutive models incorporating volume change relate deformation state variables with stress state variables (Mitchell and Soga, 2005). Development of a volume change model for unsaturated soils requires applying one of the governing parameters, i.e., water content or suction, as stress state variables (Gould et al., 2011). The volume change models can be depicted in the form of a 3D state surface (constitutive surface), but in order for a surface to be considered as a constitutive surface, its uniqueness needs to be verified through a series of different state path tests on identical samples. The uniqueness of the state surface can be established provided that the surface is path independent (Fredlund and Rahardjo, 1993). **Figure 1** presents a path independent constitutive surface for a typical unsaturated soil. Starting from the initial state point and taking any of the three paths (A, B or C) the state paths end up converging to a sufficiently similar final state point.

In unsaturated soils, hysteresis causes difficulties in developing a state surface that is completely unique. A solution proposed for this problem is limiting the state surface to either an always increasing or decreasing stress state (Fredlund and Rahardjo, 1993). As a result, developing a unique surface only for loading/drying (increase in net stress/suction) and another surface for unloading/wetting (decrease in net stress/suction) is required. This limitation would restrict the state surface to only representing a monotonic volume change, which is unique only if the volume either increases or decreases due to changes in stress state variables.

In principle, any variable with the potential of considerable effect on the mechanical behavior can be taken as a state variable (Lu, 2008). Therefore, both suction and water content could be considered as a state variable since these could influence the volume change of soils (Fredlund and Rahardjo, 1993; Lu, 2008). Conventionally, a combination of the net stress and matric suction is used to explain the mechanical behavior of unsaturated soils (Ng and Menzies, 2007), such as Alonso et al. (1990), and Wheeler and Sivakumar (1995) model. Measurement of suction is an inevitable part in the application of such models. This requires specialized equipment not commonly available in most geotechnical laboratories, and very much so in industrial laboratories.

In order to be widely accepted, a framework must be practical, cost effective, and be furthermore supported by a robust theoretical basis (Fredlund and Rahardjo, 1993). With these goals in mind, research works such as Heath et al. (2004), Gould et al. (2011) and Kodikara (2012), have been undertaken to develop a new framework for addressing these requirements. Due to the widespread use of water content results in industry and every-day engineering practice; the use of water content as a state variable has been theoretically verified and is also practically preferred (Lu, 2008). Heath et al. (2004) attempted to develop a model to determine the behavior of unsaturated granular materials without the need for suction measurements, by combining the relationship between Bishop's parameter (χ_w) and suction proposed by Khalili and Khabbaz (1998) with Bishop (1960) and Van Genuchten (1980) models to relate water content to suction. Heath et al. (2004) model's input parameters include void ratio, moisture ratio (product of gravimetric water content and specific gravity), and other model parameters obtainable from conventional monotonic triaxial tests, with no need for suction measurement. Gould et al. (2011) developed a model and a state surface in the space of void ratio-gravimetric water content-net stress to predict the volumetric behavior of expansive soils during shrinkage, which is only applicable to soils in environmentally stabilized state after a significant number of wet/dry cycles. In their work, void ratio was taken as the deformation state variable and net stress and gravimetric water content were taken as stress state variables. The most recent gravimetric water content-based framework was proposed by Kodikara (2012), referred to as Monash Peradeniya Kodikara (MPK) framework, to explain the volumetric behavior of unsaturated soils.

The MPK framework considers the net stress (p), void ratio (e) and moisture ratio (e_w, moisture ratio or normalized gravimetric water content) as the state variables. In the MPK framework, a number of compaction curves (in the loaded state) obtained from a range of compaction pressures (net stress) form a state surface in the space of e-e_w-p that is called the Loading-Wetting State Boundary Surface (LWSBS). This surface illustrates the loosest state a compacted soil can achieve under loading and/or wetting (Islam and Kodikara, 2015). The uniqueness of this surface for unsaturated fine-grained soils has been verified through several state paths of loading, unloading and wetting, as well as swelling/collapse due to wetting. Development and verification of the LWSBS was done without accounting for suction as an independent stress state variable. However, the incorporation of suction in the e-e_w-p space was also investigated in order to present a thorough image of the hydro-mechanical volume change behavior within the MPK framework (Islam, 2015).

The theory behind using the gravimetric water content as a state variable is the fact that for a single type of soil at a constant net stress, gravimetric water content and suction are related to each other via the soil water characteristics curve (Gould et al., 2011). In other words, since there is a single void ratio-gravimetric water content relationship for any chosen net stress that determines the corresponding suction, gravimetric water content can be used in place of suction as an independent stress state variable. Kodikara (2012) theoretically justified the selection of state variables (e, e_w and p) using the simplified form of an equation that gives the energy input to unsaturated soils through changes in net stress proposed by Houlsby (1997). Experimental results of Gould et al. (2011) and Fleureau et al. (2002) reported that in an environmentally stabilized state, moisture ratio does not show hydraulic hysteresis with void ratio. A possible explanation for these reported data is that the significant hysteresis both moisture ratio and void ratio show with suction may be eliminated when these two variables are considered together (Kodikara, 2012). This, at least for the post-environmental stabilization conditions, solves an important disadvantage of the conventional suction based models, i.e., restricting a constitutive surface to the condition of monotonic volume change.

1.2 The Current Research

The magnitude of suction is significantly lower in granular materials as compared with fine-grained materials. However, past studies not only indicate the influence of suction in the behavior of the unsaturated granular materials, but also showed the necessity of a simple and accurate framework for developing constitutive models to predict their behavior. Settlements in compacted granular material such as embankments constructed using granular materials, which are susceptible to precipitation or flooding (wetting), indicate the need for more research in the behavior of the unsaturated granular materials.

In this research, for the first time, a model for prediction of a loading-wetting state surface for granular materials is presented that was developed using the well-known compaction procedure. The model was subsequently verified and the uniqueness of the developed surface was evaluated.

Two important attributes of the developed model were: a) obtaining the model parameters through basic geotechnical tests, and b) explaining and predicting the volumetric behavior of granular materials in which internal friction and aggregate interlock govern the volumetric behavior, in contrast to fine materials in which suction is the dominant internal force. This research is a step forward in bridging the gap between unsaturated soil mechanics research and current industry practice of using unsaturated soil mechanics theories, as well as expanding the knowledge on the volumetric behavior of unsaturated recycled granular materials.

2 Experimental Program

In this section, firstly properties of the materials used in the experimental program are presented and compared with typical granular quarry materials. Subsequently, the experimental approach for selecting a suitable method of compaction for sample preparation is explained. Finally, the equipment and the testing procedure for obtaining the model parameters and that for model verification are described.

2.1 Materials

The recycled granular materials used in this research were crushed brick (CB) and excavation waste rock (WR), which are typically used as base and sub-base course in road construction in the state of Victoria, Australia. CB and WR were collected from a recycling facility in Melbourne. **Table 1** shows the geotechnical properties of the CB and WR in comparison with typical granular quarry materials. Figure 2 presents the particle size distribution (PSD) of CB and WR and also reports on other properties including maximum particle size (D_{max}), coefficient of uniformity (Cu) and coefficient of curvature (Cc).

Results presented in **Table 1**, as well as previous research indicate that CB and WR have physical properties comparable to typical granular materials. The water absorption for CB and WR was reported respectively as 6.25 and 3.44, which is less than the maximum water absorption normally expected for quarry materials of around 10 (Arulrajah et al., 2013). In addition, Los Angeles abrasion for the CB and WR was reported as 36 and 21 respectively, which is within the threshold for quarry materials with a maximum of 40 (Arulrajah et al., 2012; Arulrajah et al., 2013). Friction angles of 48º and 51º was reported for CB and WR, respectively which are greater than the minimum friction angle expected for typical quarry material of 35º (Arulrajah et al., 2013). A more precise observation of the material indicates that in contrast to WR particles, micropores are observed in CB particle, the existence of which could potentially result in compacted CB samples having dual porosity. However, soil water characteristics curves (SWCC) of CB blends presented by Azam et al. (2013) and Azam et al. (2014) are similar to those of a granular material with single porosity.

2.2 Selection of the Compaction Method

Impact (standard/ modified Proctor) and static methods of compaction are the most commonly used procedures for laboratory compaction. In order to select between impact and static methods of compaction, the post-compaction PSD and soil-water characteristics of the compacted samples were studied. Details of the testing method for this investigation are reported in Yaghoubi et al. (2017). After densifying the samples to the same target density (**Table 1**), the impact and static specimens were extruded from the molds and dried in the oven. Next, sieve analysis was done to compare the changes in post-compaction PSD of the specimens. Using the data obtained from compaction and sieve analysis, the Aubertin et al. (2003) and Perera et al. (2005) predictive models were used for estimation of the SWCC of the impact and static samples. These methods are applicable for estimation of SWCC of granular materials.

A difficulty in working with granular materials is preparing identical samples/specimens. In spite of the common procedures used for sample splitting, such as quartering or using riffles, preparing smaller batches of coarse material with reasonably similar PSD is difficult. In this research, sample reconstitution was undertaken to resolve this issue. For each material three closely identical samples were prepared using a riffle splitter. Sieve analysis was done on the samples and the medial gradation of the three test was considered as the nominal PSD of the samples. Based on this PSD, three portions were defined for particles: larger than 9.5 mm, between 9.5 and 2.36 mm, and smaller than 2.36 mm. All the available material was then split using control sieves with 9.5 and 2.36 mm aperture sizes. Finally, the measured portions were used to reconstruct the test samples.

2.3 Compaction Equipment and Tests

To obtain the group of compaction curves (in the loaded state) for developing the loading-wetting surface, static compaction was conducted on samples with different gravimetric water contents (hereafter referred to as water content or GWC) ranging from approximately half the OWC to saturation condition in 2-3% increments. Samples were compacted under pressures of 100, 200, 500, 1000, 2000, and 4000 kPa in order to generate the static compaction curves. Since there is no specific standard for the measurement of volume change behavior in granular unsaturated soils, the overall procedure of the proposed test was based on ASTM-D2435 (2011) with some modifications to fit the load frame capacity. For instance, according to ASTM-D2435 (2011), and considering the D_{max} of the materials being 19 mm, the minimum diameter of the compaction mold was required to be 500 mm. With this loading surface, the maximum compaction pressure that can be applied by a loading frame with 100 kN capacity would be 0.5 MPa. This is insufficient for densifying the sample to MDD values obtained from modified Proctor method. Based on the previous test results on CB presented in Yaghoubi et al. (2017), a pressure between 10 MPa to 12 MPa was required for that purpose and a pressure of 4 MPa results in a sample with a dry density of 90-93% MDD. Considering the load frame capacity, a thickness of 50 mm and a diameter of 125 mm was selected for the specimens, resulting in a diameter to thickness ratio of 2.5 in accordance with ASTM-D2435 (2011). **Figure 3** shows details of the testing equipment and the compaction mold.

Two different loading rates depending on the GWC of the sample were selected for reaching the target constant net stress required for compaction. Considering the OWCs corresponding to modified proctor compaction of 10.8% for CB and 5.7% for WR, loading rates of approximately 500 kPa/min and 50 kPa/min were applied on samples with GWC lower or higher than their OWCs respectively. The target static pressure was then kept constant until no further deformation was observed in the sample (after procedures explained in Olson and Langfelder (1965) and Islam and Kodikara (2015)). At the end of the compaction procedure, the final thickness of the specimen was measured. Subsequently, the specimen was extruded from the mold as quickly as possible, weighed and placed in the oven for determination of the water content. During compaction, drainage was allowed from the top of the loading plate as is the case in impact method. However, a filter paper was used to prevent possible migration of fines during the drainage.

2.4 State Path Tests

The same mold with the capability for controlled injection of water from the top and sides of the sample was used for conducting the loading-wetting (LW) state paths. Loading was done using a UTM-100 loading system (**Figure 3**), and wetting was achieved by injecting the calculated amount of water through the top and side openings of the loading plate and mold using a graded syringe. In the LW state paths, a constant pressure was applied on the samples with pre-determined initial water content. Once no further displacement occurs, the calculated amount of water corresponding to a 2% increase in the water content was added, while the pressure was kept constant during the whole wetting procedure. Following each injection, the openings were covered with cellophane sheets in order to prevent evaporation. Water content was increased step-by-step until no more water could be added to the sample (saturation state). The displacement of the top plate was recorded while taking the state paths to calculate the volume of the sample in each stage. At the end of the state path, the soil sample was extruded from the mold as quickly as possible for determination of the final GWC, and the initial GWC was then back calculated to ensure the accuracy of calculations and the wetting procedure.

2.5 Oedometer Tests

In order to generate the compression curves of void ratio-vertical stress for specimens from a relatively loose state, a procedure similar to ASTM D2435 (2011), with slight modifications, was used. The objective of this procedure was to determine the compression indices of CB and WR in dry and saturated conditions as discussed in Section 4. The testing equipment and the compaction mold described in Section 2.3 were used with an incrementally applied controlled-stress loading schedule of 100, 200, 500, 1000, 2000 and 4000 kPa. Each test specimen was kept under each constant loading stage until no or very minor deformation was recorded. A data logger was used for the collection of both load and deformation data.

3 Developing the State Surface

Developing the constitutive surface was undertaken by producing a family of $e\text{-}e_w$ curves using a compaction procedure, therefore making the selection of a proper compaction method important. **Figure 4 (a)** shows the before compaction PSD of CB, and the similarity of after static and impact compaction PSDs, and **Figure 4 (b)** indicates the small difference in the estimated SWCCs of impact and static specimens. Therefore, it was expected that using either the impact or static methods of compaction for specimen preparation would result in a similar unsaturated volumetric response. As a result, the static method of compaction was selected over the more popular modified Proctor (impact) method due to better precision and higher control in the testing procedure.

Figure 5 shows the group of curves for CB obtained through static compaction under various stress levels in ρ_d-w-p space. This surface indicates the reduction in the maximum achievable post-compaction GWC when increasing the compaction pressure from 100 kPa to 4000 kPa. During the compaction, drainage was allowed to prevent the build-up of pore air and water pressure. Otherwise, the actual net stress on the sample would be lower than the target net stress resulting in less densification of the sample. For the same reason, a lower loading rate was used for the compaction of samples wetter than OWC. In this research, the loading rates of 500 and 50 kPa/min were applied for samples dryer or wetter than OWC, respectively. In **Figure 5** the constant water content contours are also shown. For developing this surface, the data corresponding to a water content of 5.5% and greater were used. This is about half the OWC of CB, and compaction at water contents lower than this in practice is unlikely.

Values of dry density can be converted into void ratio (e) which is commonly used as the deformation state variable in soil constitutive models. Values of e and Δe give the deformation for any thickness of a geotechnical layer, and values of GWC can be normalized by multiplying it into

G_s. The product GWC and G_s is the moisture ratio (e_w), which is equal to void ratio when the soil is fully saturated. Conducting these conversions, the family of curves are presented in **Figure 6** in a plane of e-e_w and in **Figure 7** as a surface in the space of e-e_w-p. In both **Figures 6** and **7** the line of S_r=1 and the line of optimums (LOO) is also shown. For the impact compaction method, LOO is a line or curve drawn by connecting the MDD point of each compaction curve obtained from a different compaction effort (Holtz et al., 2011). For the static compaction method, the LOO can be drawn by connecting the point on each curve from where no more increase in dry density occurs (i.e. MDD). LOO is defined as a boundary between the dry side of compaction curve where air can easily exit the soil and the wet side of compaction curve where air is trapped due to rapid soil loading (Islam and Kodikara, 2015). In the framework of this research, LOO was used to determine the ζ parameter as the ratio of e_w on LOO to the corresponding e_w on the S_r=1 line (refer to **Figure 6**).

In **Figures 6** and **7**, a noticeable point in the e-e_w curves is the initial increase in void ratio (decrease in the dry density) at the dry side of the curves. This is evident at the dry end of the compaction curves in **Figure 5**, and was more visible in the curves corresponding to lower stress levels. Similar trends were reported by El-Mountassir et al. (2014) and Islam and Kodikara (2015). Voids in a block of soil consist of two types of pores, being inter-particle pores and intra-particle pores. In samples with low water contents, it is known that the water fills the intra-particle pores first, and subsequently fills the inter-particle pores (El-Mountassir et al., 2014; Romero et al., 2011). The GWC at the dry side of the curves may be sufficient to saturate the intra-particle pores, but not enough to develop a meniscus film in the inter-particle pores. Lack of meniscus film results in no suction effect, despite the fact that high suction values are theoretically expected at low S_r values. Suction forces are known for resistance against external loading by pulling the particles toward one another (Alonso et al., 1990; Likos and Lu, 2004). Increasing the water content between low S_r ranges of 20% and 30% resulted in the formation of menisci which made the suction forces effective. Suction values are normally low in granular materials, yet sufficient to influence the compaction curves obtained in low stress levels. For the S_r value of approximately 30% to saturation, as suction forces diminish eventually, the e-e_w curves followed the typical trend and reduction of void ratio was observed as moisture ratio increased. Settlement (reduction of void ratio) continued until reaching the minimum void ratio (MDD). At this stage, the extra water added to the sample drained and constant deformation readings resulted in no more reduction of void ratio. As a result, the void ratio of the sample at this point (e_{wm}) was almost the same as the void ratio corresponding to moisture ratio at saturation (e_{ws}).

4 Model Development

In order to develop a model to predict the e-e_w curves, the plot of **Figure 6** was carefully observed. **Figure 8** shows close-up images of the curves corresponding to p = 100 kPa and p = 1000 kPa, selected from **Figure 6**, and introduces some of the parameters used in the predictive model. In this figure, connecting the data points achieved by conversion of the corresponding compaction curve data forms the continuous line, and the dashed line is the polynomial trend-line drawn using these points. Both curves significantly coincided from the dry side with a water content of 7.5% (e_w = 0.2) up to moisture ratio of e_{wm}. In reality, for moisture ratios greater than e_{wm}, negligible changes occurred in void ratio values (Δe of less than 0.001) until the soil was fully saturated.

The trend-line between e_w of 0.2 and e_{wa} (average value of e_{wm} and e_{ws}) is similar to a y=cos(x) function where $0<x<\pi$. Considering $e_{wd} < e_w < e_{wa}$ and $e_d < e < e_s$ (=e_{wm}), the relationship can be explained using Equation 1:

$$e = \left(\frac{e_d - e_s}{2}\right) \cos\left[\left(\frac{\pi}{e_{wa} - e_{wd}}\right)(e_w - e_{wd})\right] + \left(\frac{e_d + e_s}{2}\right) \quad (1)$$

where e and e_w are void ratio and moisture ratio of interest respectively, e_{wa} is the average of e_{wm} and e_{ws} (Equation 2), e_{wd} is moisture ratio at the dry end, e_s is void ratio at saturation (Equation 3), and e_d is void ratio at the dry end (Equation 4).

$$e_{wa} = 0.5\,(1 + \zeta)e_s \quad (2)$$

$$e_s = e_{s0} - \lambda_s \ln(\frac{p}{p_{low}}) \quad (3)$$

$$e_d = e_{d0} - \lambda_d \ln(\frac{p}{p_{low}}) \quad (4)$$

Here, ζ is the ratio of e_{wm}/e_{ws} (=0.81 for CB), λ_s is the slope of compression line at saturation, λ_d is the slope of compression line at e_{wd}, p_{low} is the lowest net stress used for developing the family of e - e_w curves (equal to100 kPa in this research), e_{s0} is the void ratio at saturation under the net stress of p_{low}, and e_{d0} is the void ratio at the dry end under the net stress of p_{low}.

Figure 9 shows the compression lines for e_w = 0.2 and e_{ws} with λ_s and λ_d of respectively 0.065 and 0.091 for CB. Evidently, the slope of the compression line was greater at dryer conditions. This was consistent with results reported by Alonso et al. (1990), and Wheeler and Sivakumar (1995) conducting load increments at zero suction (saturation) and greater values of suction (dryer conditions). **Figure 9** also shows that a linear relationship can be assumed between "e" and the natural logarithm of "p" (as was proposed in Equations 3 and 4).

The void ratios predicted using Equation 1 are presented in **Figure 10 (a)** in comparison with the measured ones in the e-e_w plane. Experimental data points are also presented in **Figure 10**. Comparison of the measured and predicted data showed that the developed model could effectively predict the compaction curves between moisture ratio of 0.2 (i.e., w ≈ 7.5%) and the saturation condition. Considering the OWC of CB being approximately 11%, this could be a practical range of water content for compacting this material in the field. The measured values of e plotted in the e-log p plane (**Figure 10 (b)**) follow the predicted values closely, which validates the assumption of a linear relationship between e and log p.

5 Verification of the Proposed Model

In order to verify the proposed model and to evaluate the uniqueness of the developed surface, two approaches were taken: a) verification through independent specimens, and b) verification through loading and wetting state paths, involving investigation of whether the paths follow the developed surface and inspection of whether the model was path independent.

5.1 Verification Using Independent Specimens

In order to validate the model, the proposed approach was used to predict e-e_w curves for WR. A number of compaction tests were conducted at the wet end of the samples under 100, 1000, 2000 and 4000 kPa to estimate ζ, which was determined to be 0.84. Also, a complete set of compaction tests were conducted to determine the compaction curves for 100 kPa and 1000 kPa net stresses for comparing the predicted and measured data. For CB with OWC of 10.8%, GWC at the dry end was 7.5% (e_{wd} = 0.20). However, for WR with a lower OWC of 5.8%, GWC at the dry end should begin with a lower percentage. For WR, a lower GWC of 3.5% (e_{wd} of 0.1) was selected for the dry end of the compaction curves, since the OWC of WR was approximately half of the OWC of CB (see Table1). Compression indices (λ_d and λ_s) were obtained through one-dimensional (1D) oedometer tests (1D compression test or constraint modulus test for unsaturated soils) on samples at e_{wd} and saturation conditions. **Figure 11** shows the compression lines for e_w = 0.10 and e_w = e_{ws}

for WR. Values of λ_s and λ_d for WR are 0.069 and 0.087, respectively. The slope of the compression line for the dry end of WR was lower than that of CB. This could be due to lower suction forces in WR, as was expected considering the lower OWC and fine content of this material. Lower suction values, and higher specific gravity of the WR particles resulted in a greater settlement of the WR samples due to gravity and self-weight compared to CB. In other words, when placing the samples inside the mold, before applying the compression loads, more settlement due to self-weight occurred in WR than did in CB. This enabled less attainable deformation to occur due to loading; hence, lower values of λ_d and λ_s. Additionally, the difference compared to CB in the slope of the compression lines for the saturation and dry conditions in WR was lower. This indicates the lower sensitivity of this material to changes in GWC which could be attributed to lower suction ranges.

Table 2 summarizes the model parameters obtained in the proposed model for CB and WR. **Figure 12** shows experimentally obtained values of "e" in e-e_w and e-log p planes in comparison with those predicted by the developed model. Predicted and measured data matched well which verified the applicability of the proposed model for WR.

5.2 Verification Using the State Paths

The proposed model aimed to predict a loading-wetting surface, which represented the loosest state that the soil had attained at a specific water content under a specific stress level. In order to verify whether the developed surface was path independent, thus constitutive, a number of state paths were defined as combinations of loading and wetting state paths. Two aims were sought in order to verify the uniqueness of the surface. First, the state paths were expected to reach the surface from a loose state due to loading, and from there follow the corresponding path through the process of wetting the sample while under a constant net stress. Second, starting from a loose point at the same water content, by conducting either a loading then wetting path or a wetting then loading path was expected to reach the same point on the surface, provided that the target GWC and p were the same.

Figures 13 (a) and **(b)** show the results of taking two loading-wetting (LW) paths on CB in e-e_w and e-log p planes. On the path shown with a continuous line, the CB sample was prepared at the GWC of 12.7% (e_w = 0.34), was loaded to 200 kPa and then wetted to saturation. The path reached the corresponding curve on the surface by loading, but it did not follow the surface through the wetting cycle. In the path shown with dashed line, the CB sample with GWC of 9.5% (e_w = 0.25) was loaded to 2000 kPa and then wetted to saturation. This LW path not only reached the curve corresponding to p = 2000 kPa by loading, but it also closely followed the surface through wetting under constant p = 2000 kPa. **Figures 13 (c)** and **(d)** show similar LW state paths for WR samples. For WR, the paths reached the corresponding curve through loading but the surface was only followed through wetting under the high net stress of 4000 kPa. During wetting under constant net pressure, reduction of the two resisting forces of suction and internal friction between particles resulted in reduction of void ratio. In the case of CB and WR with low suction values internal friction was the main factor resisting against deformation. When the LW path started from a dry loose state, wetting the sample under a constant net stress caused a noticeable deformation. This was mainly attributed to the lubricating effect of water and partly due to reduction of suction (continuous LW path in **Figure 13 (b)**). In contrast, not much deformation due to wetting was observed when the LW path started from a wet loose state. This could be because at the wet state, lubrication had already been accomplished during sample preparation and suction values were close to zero (continuous LW path in **Figure 13 (a)**).

Similar behavior as LW state paths was observed by taking a Loading-Wetting- Loading-Wetting (LWLW) state path. **Figure 14** shows a CB sample compacted under p=50 kPa at e_w = 0.21 (point O), then loaded to p = 200 kPa (point A), then wetted to e_w = 0.31 (point B), then loaded to p = 500 kPa (point C), and finally wetted to saturation under constant pressure of 500 kPa (point D). Both loading paths (OA and BC) reached the corresponding curve among the family of e-e_w curves by loading. However, the e-e_w curves were not followed through the second wetting path (CD). The reason for the wetting path of AB being relatively close to the e-e_w curve corresponding to p = 200kPa could be the small change in e_w (Δe_w = 0.1). The continuous LW path in **Figure 13 (a)** indicates that the p = 200 kPa curve would not be followed if the wetting continued under p = 200 kPa from point B in **Figure 14**.

Taking several LW state paths with initial water contents of 3.9% to 13.4% for CB and WR and constant net stresses of 100 kPa to 4000 kPa revealed that the predicted surfaces for CB and WR are unique with respect to loading, but these are only unique with respect to wetting in stress levels greater than 2000 kPa. This was a net stress value that resulted in samples with MDD of approximately 90% of the modified Proctor method. In practical terms, in order for a compacted base and sub-base or embankment fill to meet the required quality control, typically a minimum of 95% MDD of modified or standard Proctor compaction must be achieved. Therefore, even though on initial inspection it seemed that the surface was inaccurate in predicting the volumetric behavior of granular materials in low stress levels, it produces accurate results at higher stress levels corresponding to practical applications of these materials, thereby confirming that the methods presented herein will aid in using granular material, in particular, recycled granular material in real world engineering problems.

The volumetric response of granular materials under low stress conditions is known to be significantly different from those under higher pressures (Macari-Pasqualino et al., 1994). High internal frictions between rough surfaced particles of granular materials and low suction forces could result in a different response in LW state paths, causing these to not follow the surface at low stress levels. The e-e_w curves were obtained through static compaction tests on identical loose samples each prepared with a moisture ratio ranging from e_{wd} to e_{ws}. In the LW state path, wetting to different moisture ratios was done on a sample that was already densified and under static net stress. Therefore, the displacement and slipping of aggregates through wetting was limited due to high internal friction assisted by particle interlocking. This resulted in lower changes in void ratio compared to what was predicted using the e-e_w curves. On the contrary, in fine materials such as kaolin, where suction plays the major role and internal friction has a significantly lower impact, the LW state paths closely follow the e-e_w curves and changes in void ratio could be predicted using the surface (Islam and Kodikara, 2015; Kodikara, 2012). Developing a model for predicting the volume change of granular material in low stress levels is under investigation as the next phase of this research.

Figures 15 (a) and **(b)** show LW (OAB) and WL (OA'B') state paths for CB in e-e_w and e-log p planes, respectively. Both state paths started from point O which was a loose state at GWC=8.7% (e_w = 0.23). In the LW path, the sample was loaded to p = 4000 kPa at constant GWC of 8.7% (point A) and then wetted to GWC of 11.5% (e_w = 0.3), leading to point B with void ratio of 0.41. In the WL path, the sample was wetted to GWC=11.4% (e_w = 0.3) under a very low stress of 2 kPa (point A') and then loaded to p = 4000 kPa at e_w = 0.3 (point B'). At B', the void ratio of the sample was 0.42 which was close to what was previously obtained from the OAB path. The void ratio corresponding to e_w = 0.3 and p = 4000 kPa on the surface was 0.41. Similar state paths were followed for WR samples (**Figures 15 (c)** and **15 (d)**) starting from a loose state at GWC=3.8% (e_w = 0.11). LW path of OAB and WL path of OA'B' ended up in void ratios of 0.43 and 0.42 at e_w= 0.31 and p = 4000 kPa respectively. At e_w = 0.31 and p = 4000 kPa the surface of WR showed a void ratio of 0.43. The fact that both these state paths reached the same point on the surface verified the uniqueness and path independence of that surface; a good outcome even though the results were limited to high stress levels and to monotonic loading and wetting at this stage.

The state paths presented in **Figures 13** to **15** show small volume changes, especially when the sample was loaded to higher stress levels. For instance, Δe due to wetting in **Figure 15 (a)** from point A to B was less than 0.01 and in **Figure 15 (c)** was approximately 0.03. Volume change due to wetting (reduction of suction) is large in fine-grained materials, especially materials in a loose condition. However, in granular materials, such as road construction materials that are normally well compacted and contain low fine contents, small volume changes occur by changes in water content (Heath et al., 2004). Nevertheless, these small volume changes eventually result in a major distress such as rutting as they accumulate, and thus should also be taken seriously.

5.3 Summary of the Proposed Procedure

The most important feature of the proposed model is the simplicity at which the input data is collected. Inputs were easily obtained through a small number of compaction tests under the pressure of p_{low}, two 1D compression tests, and a few random compaction tests for estimating the ζ ratio, as well as validation of predicted curves. **Table 3** presents a list of input data required for using the model (Equations 1 to 4), and the tests needed for determining these. The first step is the selection of e_{wd0} of interest, and conducting a few trial compaction tests in order to estimate e_{ws0}. The tests listed in **Table 3** can be used as a guide for obtaining other input parameters. Since preparing identical specimens using granular materials is difficult and brings about uncertainties, it is recommended that repetitive tests are conducted and the average values used as the input parameters as presented in the last column of Table 3.

6 Conclusions

In this paper, a model was proposed for prediction of the volume change behavior of unsaturated granular materials through changes in the stress level or the moisture condition. First, a loading-wetting surface was developed in the space of void ratio-moisture ratio–net stress. Subsequently, an experimental procedure was proposed aiming to facilitate the developing of such a surface for granular materials. The input parameters of the proposed model could be obtained through routine geotechnical testing methods and no specialized equipment was required.

The model was developed and evaluated based on a complete set of data encompassing a wide range of moisture ratio and net stress for CB. Firstly, WR as an independent material was used to verify the procedure by comparing the experimentally obtained and predicted values of void ratio. Secondly, the uniqueness of the developed surface was evaluated by conducting combinations of loading and wetting state paths. Results showed that the surface was unique in monotonic loading for both low and high stress levels. However, the uniqueness of the surface for wetting (reduction of suction) paths was only verified in high stress levels (greater than 2000 kPa).

An application of this model could be the prediction of the void ratio (density) of the unbound pavement layers compacted at a pre-determined water content under known compaction energy. Another application of the model could be the estimation of the settlement of a granular geotechnical layer supporting the load of a footing, and for example where the footing was wetted through precipitation. Research in this area will continue focusing on investigating more state paths such as loading-unloading-wetting, and developing a model for prediction of wetting paths under low stress levels. These will be discussed in a future publication by the authors.

7 Notations

The following symbols are used in this paper:

CB = crushed brick

D_{max} = maximum particle size

e = void ratio

e_d = void ratio at the dry end

e_{d0} = void ratio at the dry end under p_{low}

e_s = void ratio at saturation

e_{s0} = void ratio at saturation under p_{low}

e_w = moisture ratio ($G_s \times$ GWC)

e_{wa} = average of e_{wm} and e_{ws}

e_{wd} = moisture ratio at the dry end

e_{wm} = moisture ratio at MDD

e_{ws} = moisture ratio at saturation

G_s = specific gravity

GWC = gravimetric water content

LOO = line of optimum

LW = loading-wetting (state path)

MDD = maximum dry density

OWC = optimum water content

p = net stress (σ-u_a)

p_{low} = the lowest net stress

S_r = degree of saturation

u_a = pore air pressure

u_w = pore water pressure

WL = wetting-loading (state path)

WR = waste rock

ζ = ratio of e_{wm}/e_{ws}

λ_d = slope of compression line at e_{wd}

λ_s = slope of compression line at saturation

ρ_d = dry density

σ = total stress

8 References

Alonso, E. E., Gens, A., & Josa, A., 1990. A constitutive model for partially saturated soils. *Geotechnique*, *40*(3), 405-430.

Arulrajah, A., Ali, M., Piratheepan, J., & Bo, M., 2012. Geotechnical properties of waste excavation rock in pavement subbase applications. *Journal of Materials in Civil Engineering*, *24*(7), 924-932.

Arulrajah, A., Piratheepan, J., Disfani, M. M., & Bo, M. W., 2013. Geotechnical and Geoenvironmental Properties of Recycled Construction and Demolition Materials in Pavement Subbase Applications. *Journal of Materials in Civil Engineering, 25*(8), 1077-1088. doi:10.1061/(ASCE)MT.1943-5533.0000652

Arulrajah, A., Disfani, M. M., Horpibulsuk, S., Suksiripattanapong, C., & Prongmanee, N., 2014. Physical properties and shear strength responses of recycled construction and demolition materials in unbound pavement base/subbase applications. Construction and Building Materials, 58, 245-257.

ASTM-D2435. 2011. Standard Test Methods for One-Dimensional Consolidation Properties of Soils Using Incremental Loading. West Conshohocken, PA: ASTM International.

Aubertin, M., Mbonimpa, M., Bussière, B., & Chapuis, R. P., 2003. A Model to Predict the Water Retention Curve from Basic Geotechnical Properties. *Canadian Geotechnical Journal, 40*(6), 1104-1122. doi:10.1139/t03-054

Azam, A., & Cameron, D., 2013. Geotechnical Properties of Blends of Recycled Clay Masonry and Recycled Concrete Aggregates in Unbound Pavement Construction. *Journal of Materials in Civil Engineering, 25*(6), 788-798. doi:10.1061/(asce)mt.1943-5533.0000634

Azam, A., Cameron, D., Gabr, A., & Rahman, M. (2014). *Matric Suction in Recycled Unbound Granular Materials.* Paper presented at the Geo-Congress 2014: Geo-characterization and Modeling for Sustainability.

Azam, A., Cameron, D., & Rahman, M., 2013. Model for prediction of resilient modulus incorporating matric suction for recycled unbound granular materials. *Canadian Geotechnical Journal, 50*(11), 1143-1158. doi:10.1139/cgj-2012-0406

Ba, M., Nokkaew, K., Fall, M., & Tinjum, J. M., 2013. Effect of Matric Suction on Resilient Modulus of Compacted Aggregate Base Courses. *Geotechnical and Geological Engineering, 31*(5), 1497-1510. doi:10.1007/s10706-013-9674-y

Bishop, A. W., 1960. *The principles of effective stress*: Norges Geotekniske Institutt.

Cameron, D. A., Azam, A. H., & Rahman, M. M., 2012. Recycled Clay Masonry and Recycled Concrete Aggregate Blends in Pavement. *Geotechnical Special Publication*, 1532-1541. doi:10.1061/9780784412121.158

Cary, C. E., & Zapata, C. E., 2011. Resilient Modulus for Unsaturated Unbound Materials. *Road Materials and Pavement Design, 12*(3), 615-638.

El-Mountassir, G., Sánchez, M., & Romero, E., 2014. An experimental study on the compaction and collapsible behaviour of a flood defence embankment fill. *Engineering Geology, 179*, 132-145.

Fleureau, J. M., Verbrugge, J. C., Huergo, P. J., Gomes Correia, A., & Kheirbek-Saoud, S., 2002. Aspects of the behaviour of compacted clayey soils on drying and wetting paths. *Canadian Geotechnical Journal, 39*(6), 1341-1357. doi:10.1139/t02-100

Fredlund, D. G., & Rahardjo, H., 1993. *Soil mechanics for unsaturated soils*: John Wiley & Sons.

Gould, S. J. F., Kodikara, J., Rajeev, P., Zhao, X. L., & Burn, S., 2011. A void ratio - water content - net stress model for environmentally stabilized expansive soils. *Canadian Geotechnical Journal, 48*(6), 867-877. doi:Doi 10.1139/T10-108

Heath, A. C., Pestana, J. M., Harvey, J. T., & Bejerano, M. O., 2004. Normalizing behavior of unsaturated granular pavement materials. *Journal of Geotechnical and Geoenvironmental Engineering, 130*(9), 896-904.

Holtz, R. D., Kovacs, W. D., & Sheahan, T. C., 2011. *An introduction to geotechnical engineering* (2nd Edition ed.). 2nd Edition, Upper Saddle River, NJ: Pearson.

Houlsby, G., 1997. The work input to an unsaturated granular material. *Geotechnique, 47*(1), 193-196.

Islam, T., 2015. *A study of volumetric behaviour of compacted clayey soils in the void ratio, moisture ratio and net stress space.* Monash University. Faculty of Engineering. Department of Civil Engineering.

Islam, T., & Kodikara, J., 2015. Interpretation of the loading–wetting behaviour of compacted soils within the “MPK” framework. Part I: Static compaction 1. *Canadian Geotechnical Journal, 53*(5), 783-805.

Khalili, N., & Khabbaz, M., 1998. A Unique Relationship of chi for the Determination of the Shear Strength of Unsaturated Soils. *Geotechnique, 48*(5), 681-687.

Kodikara, J., 2012. New framework for volumetric constitutive behaviour of compacted unsaturated soils. *Canadian Geotechnical Journal, 49*(11), 1227-1243. doi:Doi 10.1139/T2012-084

Likos, W. J., & Lu, N., 2004. Hysteresis of capillary stress in unsaturated granular soil. *Journal of*

Engineering Mechanics, 130(6), 646-655.

Lu, N., 2008. Is matric suction a stress variable? *Journal of Geotechnical and Geoenvironmental Engineering, 134*(7), 899-905.

Macari-Pasqualino, E. J., Runesson, K., & Sture, S., 1994. Response prediction of granular materials at low effective stresses. *Journal of Geotechnical Engineering, 120*(7), 1252-1268.

Mitchell, J. K., & Soga, K., 2005. Fundamentals of soil behavior.

Ng, C. W., & Menzies, B., 2007. *Advanced unsaturated soil mechanics and engineering*: CRC Press.

Olson, R., & Langfelder, L., 1965. Pore Water Pressure in Unsaturated Soils. *ASCE-Journal of the Soil Mechanics and Foundation Division, 91*(4), 127-150.

Perera, Y., Zapata, C., Houston, W., & Houston, S., 2005. Prediction of the Soil Water Characteristic Curve Based on Grain-Size-Distribution and Index Properties. *Advances in pavement engineering (ed. EM Rathje), Geotechnical Special Publication, 130,* 49-60.

Rahman, M. A., Imteaz, M., Arulrajah, A., & Disfani, M. M., 2014. Suitability of recycled construction and demolition aggregates as alternative pipe backfilling materials. *Journal of Cleaner Production, 66,* 75-84.

Romero, E., Della Vecchia, G., & Jommi, C., 2011. An insight into the water retention properties of compacted clayey soils. *Geotechnique, 61*(4), 313-328.

Suddeepong, A., Intra, A., Horpibulsuk, S., Suksiripattanapong, C., Arulrajah, A., & Shen, J. S., 2018. Durability against wetting-drying cycles for cement-stabilized reclaimed asphalt pavement blended with crushed rock. *Soils and Foundations, 58(2), 333-343*.

Suksiripattanapong, C., Kua, T.-A., Arulrajah, A., Maghool, F., & Horpibulsuk, S., 2017. Strength and microstructure properties of spent coffee grounds stabilized with rice husk ash and slag geopolymers. *Construction and Building Materials, 146, 312-320*.

Van Genuchten, M. T., 1980. A closed-form equation for predicting the hydraulic conductivity of unsaturated soils. *Soil Science Society of America Journal*, *44*(5), 892-898.

Wheeler, S. J., & Sivakumar, V., 1995. An elasto-plastic critical state framework for unsaturated soil. *Geotechnique*, *45*(1), 35-53.

Wu, Y., Guo, Y., & Zhang, X., 2009. *Application of Recycled Brick-Stone Aggregate in Road Base*. Paper presented at the Proceedings of 2009 GeoHunan International Conference. http://www.scopus.com/inward/record.url?eid=2-s2.0-71549153190&partnerID=40&md5=13cc5d5f0f9261680ad7648f774f13d5

Yaghoubi, E., Disfani, M. M., Arulrajah, A., & Kodikara, J., 2016. Impact of Compaction Methods on Resilient Response of Unsaturated Granular Pavement Material. *Procedia Engineering, 143*, 323-330. doi:http://dx.doi.org/10.1016/j.proeng.2016.06.041

Yaghoubi, E., Disfani, M. M., Arulrajah, A., & Kodikara, J., 2017. Impact of compaction method on mechanical characteristics of unbound granular recycled materials. *Road Materials and Pavement Design*, 1-23. doi:10.1080/14680629.2017.1283354

List of Tables:

List of Figures:

net stress to saturation in e-e_w plane, (d) same state path as (c) in e-log p plane

Figure 14. LWLW State path for CB, loading to p=200 kPa, wetting to GWC = 11.9%, loading to p = 500 kPa and wetting to saturation: (a) changes in stress states of p and e_w (b) the state path in e-e_w plane, (c) the state path in e-log p plane

Figure 15. Reaching the same point through LW and WL state paths: (a) loading CB samples from a loose state at GWC = 8.7% to 4000 kPa and wetting to GWC = 11.4% versus wetting in a loose state to GWC = 11.5% and then loading to 4000 kPa in e-e_w plane, (b) same state paths as (a) in e-log p plane, (c) loading WR samples from a loose state at GWC = 3.8% to 4000 kPa and wetting to GWC = 10.8% versus wetting in a loose state to GWC = 11.1% and then loading to 4000 kPa in e-e_w plane, (d) same state paths as (c) in e-log p plane

Table 1. Geotechnical properties of CB and WR used in this research

Property	CB	WR	Typical quarry materials (after Arulrajah et al. (2013))
Specific gravity (fine fraction), G_s of fine	2.61	2.88	>1.96
Specific gravity (coarse fraction), G_s of coarse	2.66	2.77	>1.96
Fine content (%) [D < 0.075 mm]	6	4	<10
Sand content (%) [0.075 < D < 4.75 mm]	45	42	-
Gravel content (%) [D > 4.75 mm]	49	54	-
Maximum particle size, D_{max} (mm)	19	19	-
Mean particle size, D_{50} (mm)	4.76	5.8	-
Soil Classification (USCS)	GW	GW	-
Maximum Dry Density, MDD (Mg/m^3)	1.99	2.22	>1.72
Optimum water content, OWC (%)	10.8	5.7	8-15
California Bearing Ratio (%)	104-116	118-143	>80

Table 2. Model parameters obtained for CB and WR

Model Parameter	CB	WR
P_{low}(kPa)	100	100
e_{d0}	0.755	0.793
e_{s0}	0.650	0.682
λ_d	0.091	0.087
λ_s	0.065	0.069
ζ (range)	0.76-0.85	0.75-0.90
ζ (average)	0.81	0.84

Table 3. Input parameters for the proposed model

Input parameter	Required test	Required No. of tests	Recommended No. of tests
e_{d0}	Compaction at the dry end under the pressure of p_{low}	1	2
e_{s0}	Compaction at the saturated end under the pressure of p_{low}	1	2
λ_d	1D compression test at the dry end	1	3
λ_s	1D compression test at the saturated end	1	3
ζ	Compaction at the saturated end under pressure of p (> p_{low})	1 (for each p)	2 (for each p)

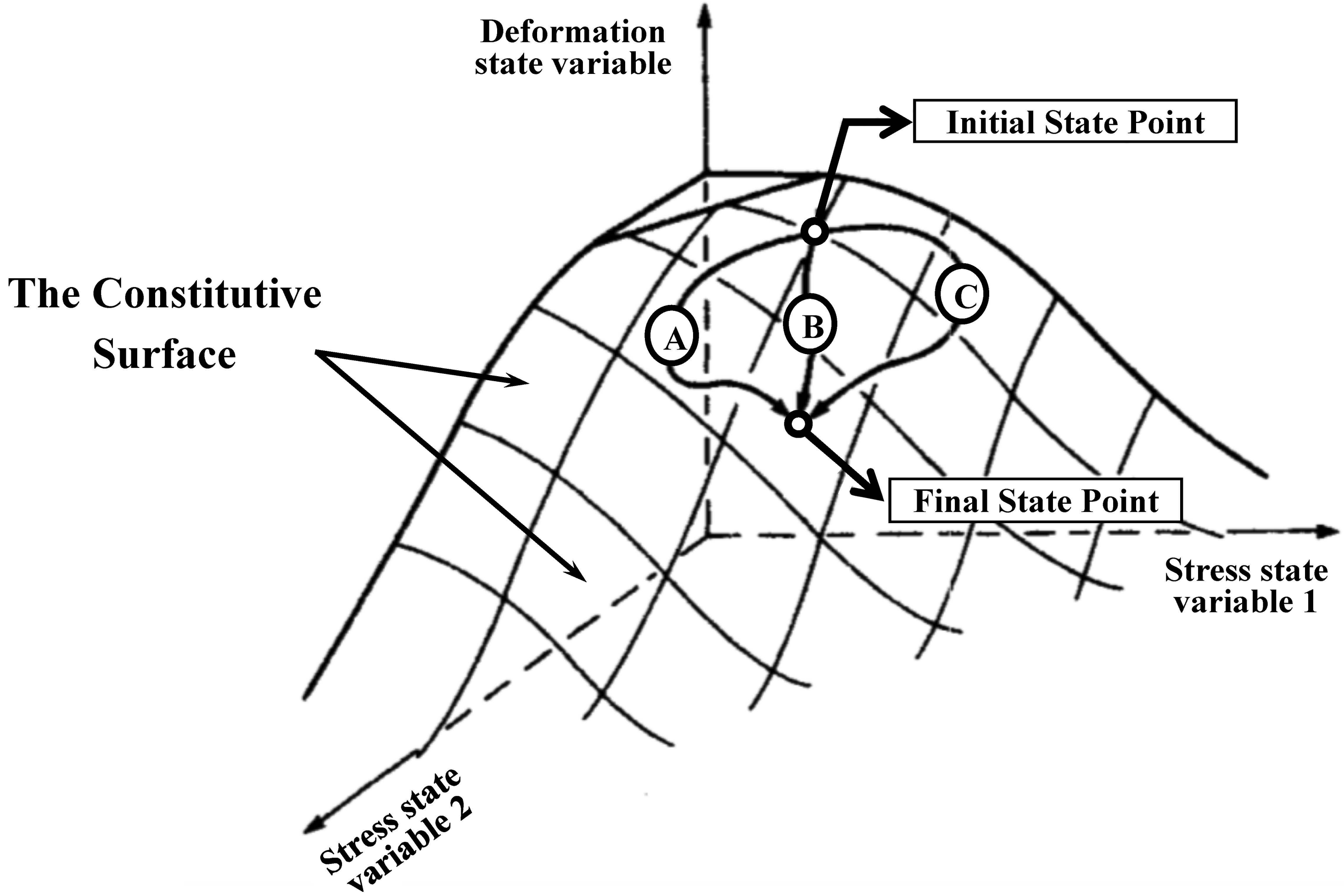
Deformation state variable
Initial State Point
The Constitutive Surface
A
B
C
Final State Point
Stress state variable 1
Stress state variable 2

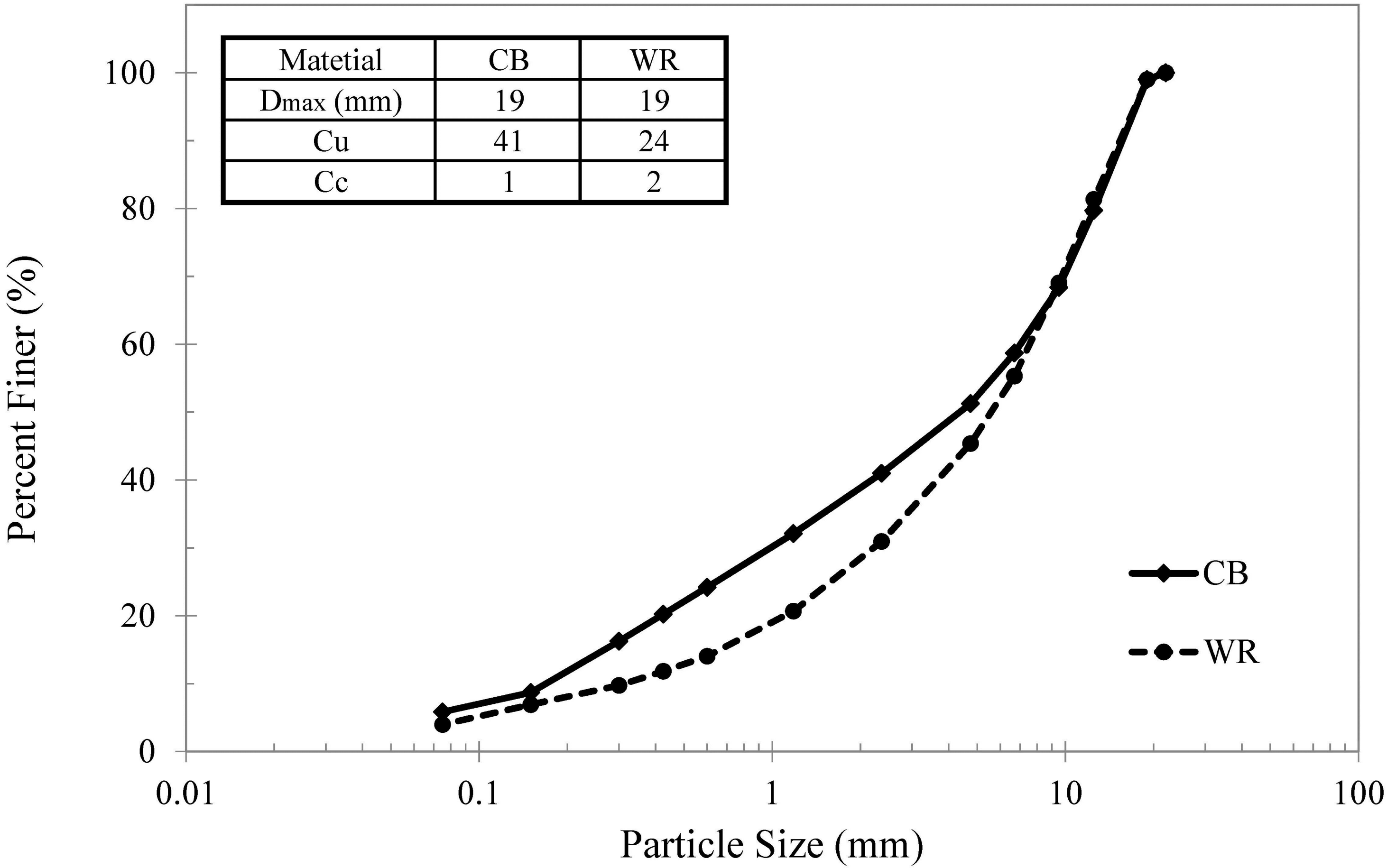
Matetial | CB | WR
Dmax (mm) | 19 | 19
Cu | 41 | 24
Cc | 1 | 2
Percent Finer (%)
0
20
40
60
80
100
0.01
0.1
1
10
100
Particle Size (mm)
CB
WR

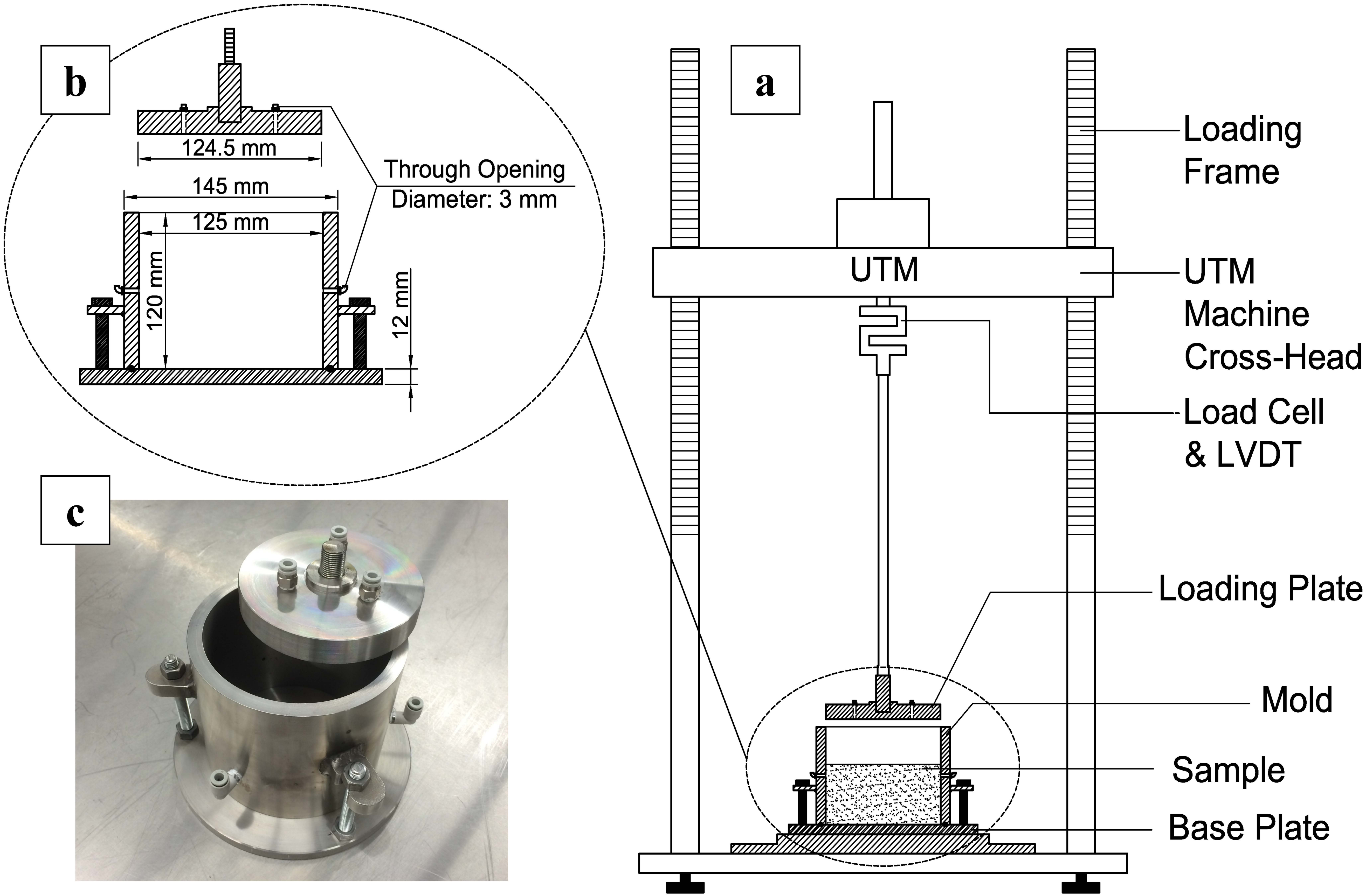
b
124.5 mm
145 mm
125 mm
120 mm
12 mm
Through Opening
Diameter: 3 mm
a
UTM
Loading
Frame
UTM
Machine
Cross-Head
Load Cell
& LVDT
Loading Plate
Mold
Sample
Base Plate
c

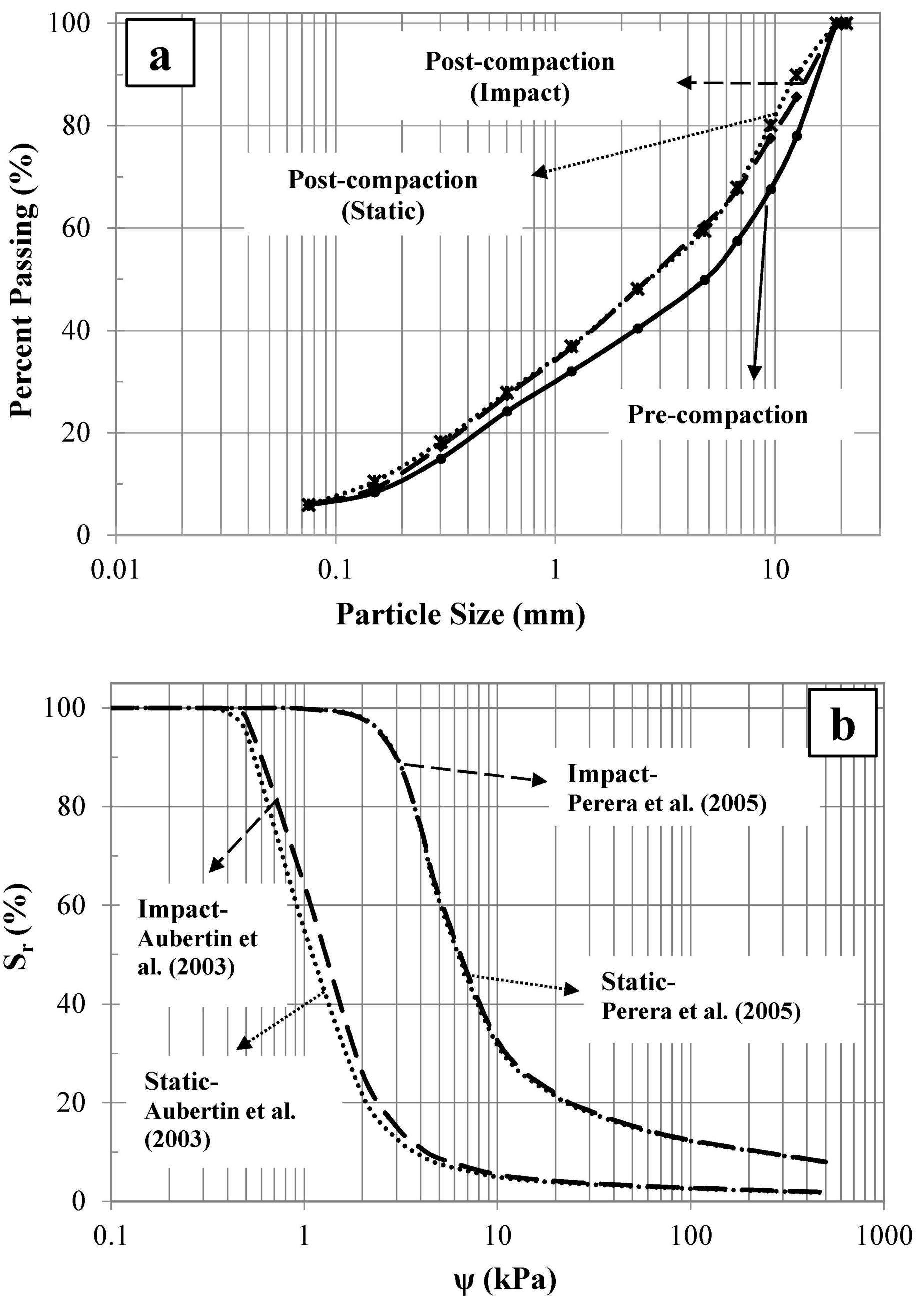
a
Post-compaction
(Impact)
Post-compaction
(Static)
Pre-compaction
Percent Passing (%)
Particle Size (mm)
100
80
60
40
20
0
0.01
0.1
1
10
b
Impact-
Perera et al. (2005)
Impact-
Aubertin et
al. (2003)
Static-
Perera et al. (2005)
Static-
Aubertin et al.
(2003)
S_r (%)
ψ (kPa)
0.1
1
10
100
1000

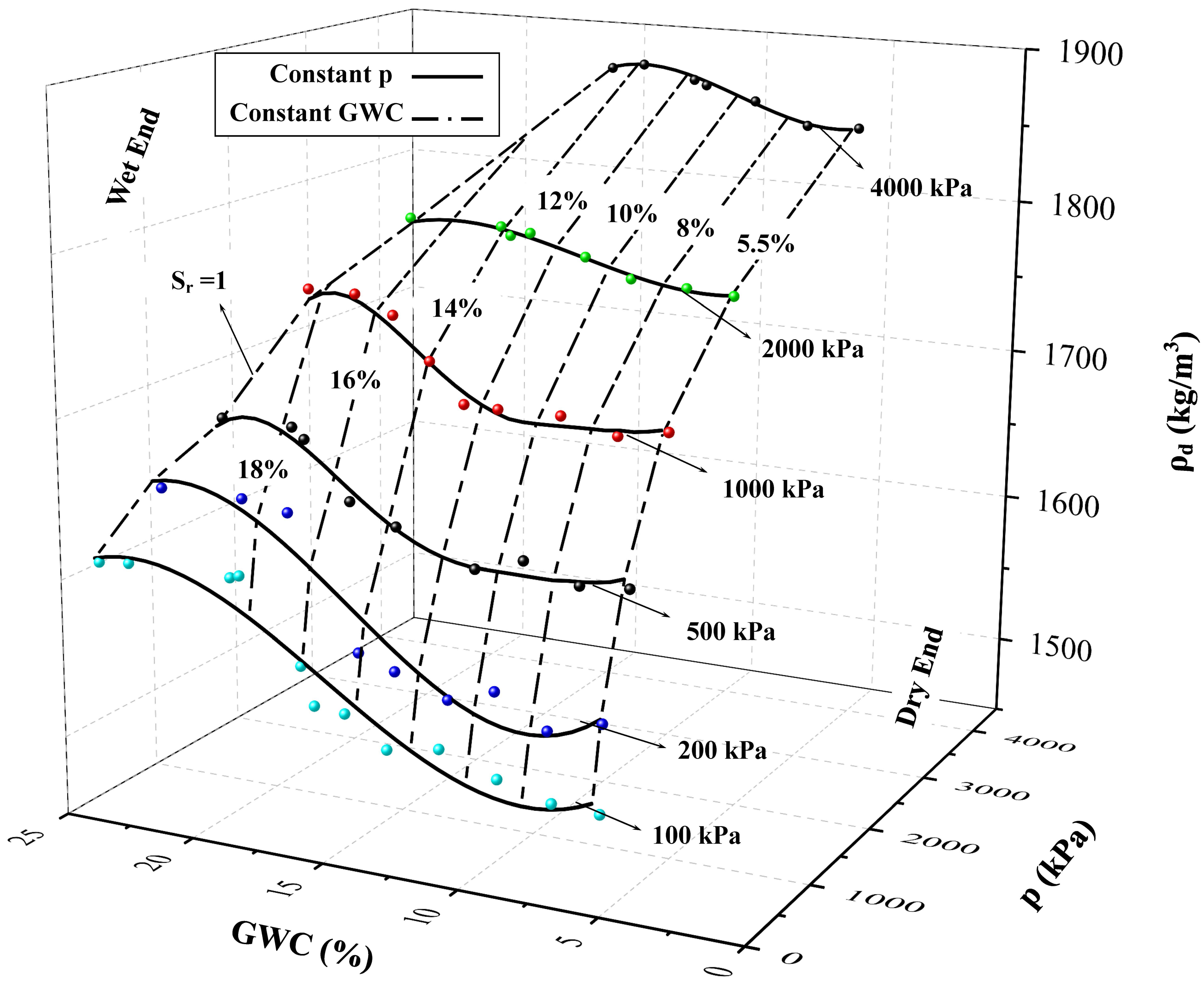

Constant p
Constant GWC
Wet End
Dry End
S_r =1
12%
10%
8%
5.5%
14%
16%
18%
4000 kPa
2000 kPa
1000 kPa
500 kPa
200 kPa
100 kPa
1900
1800
1700
1600
1500
ρ_d (kg/m^3)
25
20
15
10
5
0
GWC (%)
0
1000
2000
3000
4000
p (kPa)

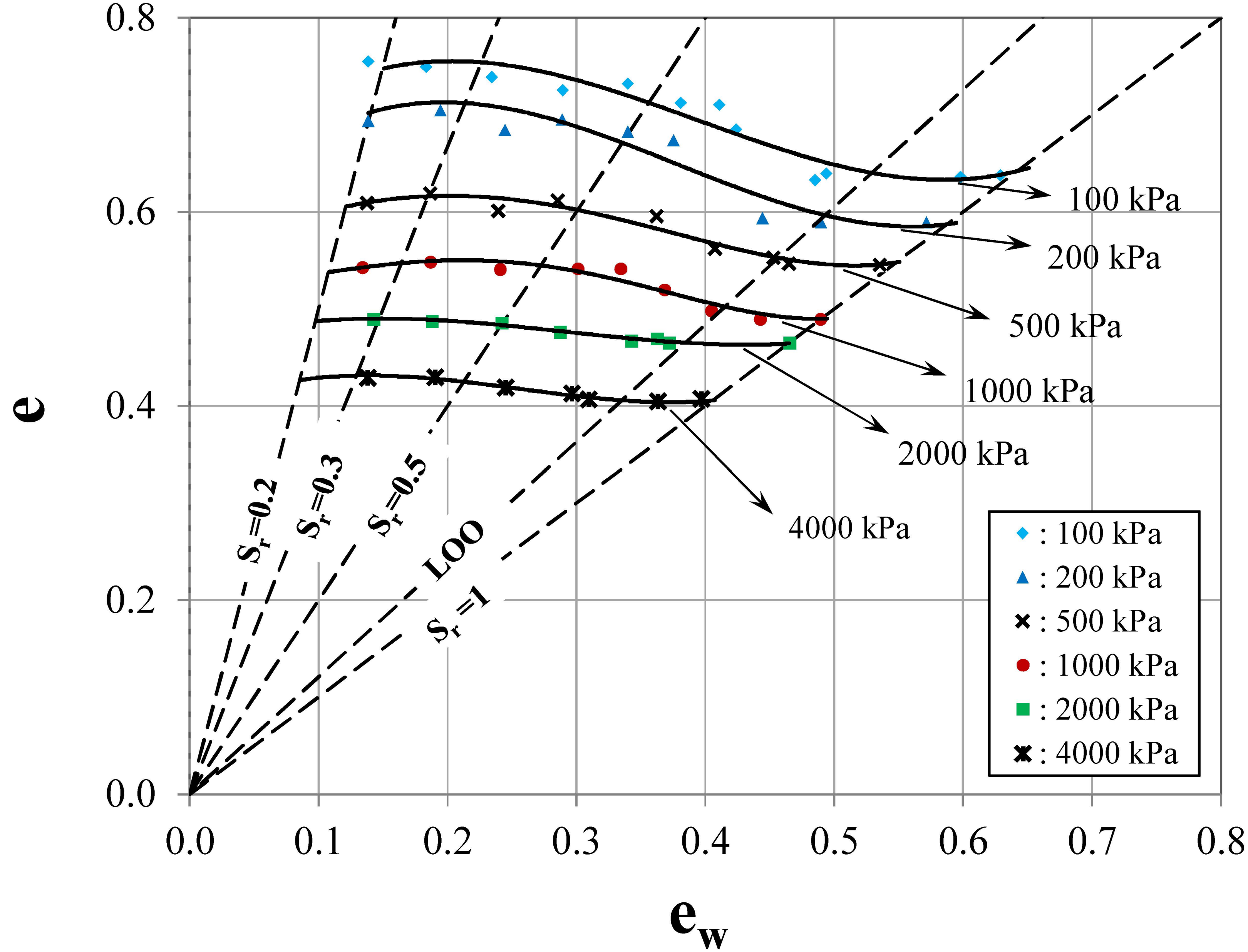

0.8
0.6
0.4
0.2
0.0
e
0.0
0.1
0.2
0.3
0.4
0.5
0.6
0.7
0.8
e_w
S_r=0.2
S_r=0.3
S_r=0.5
LOO
S_r=1
100 kPa
200 kPa
500 kPa
1000 kPa
2000 kPa
4000 kPa
: 100 kPa
: 200 kPa
: 500 kPa
: 1000 kPa
: 2000 kPa
: 4000 kPa

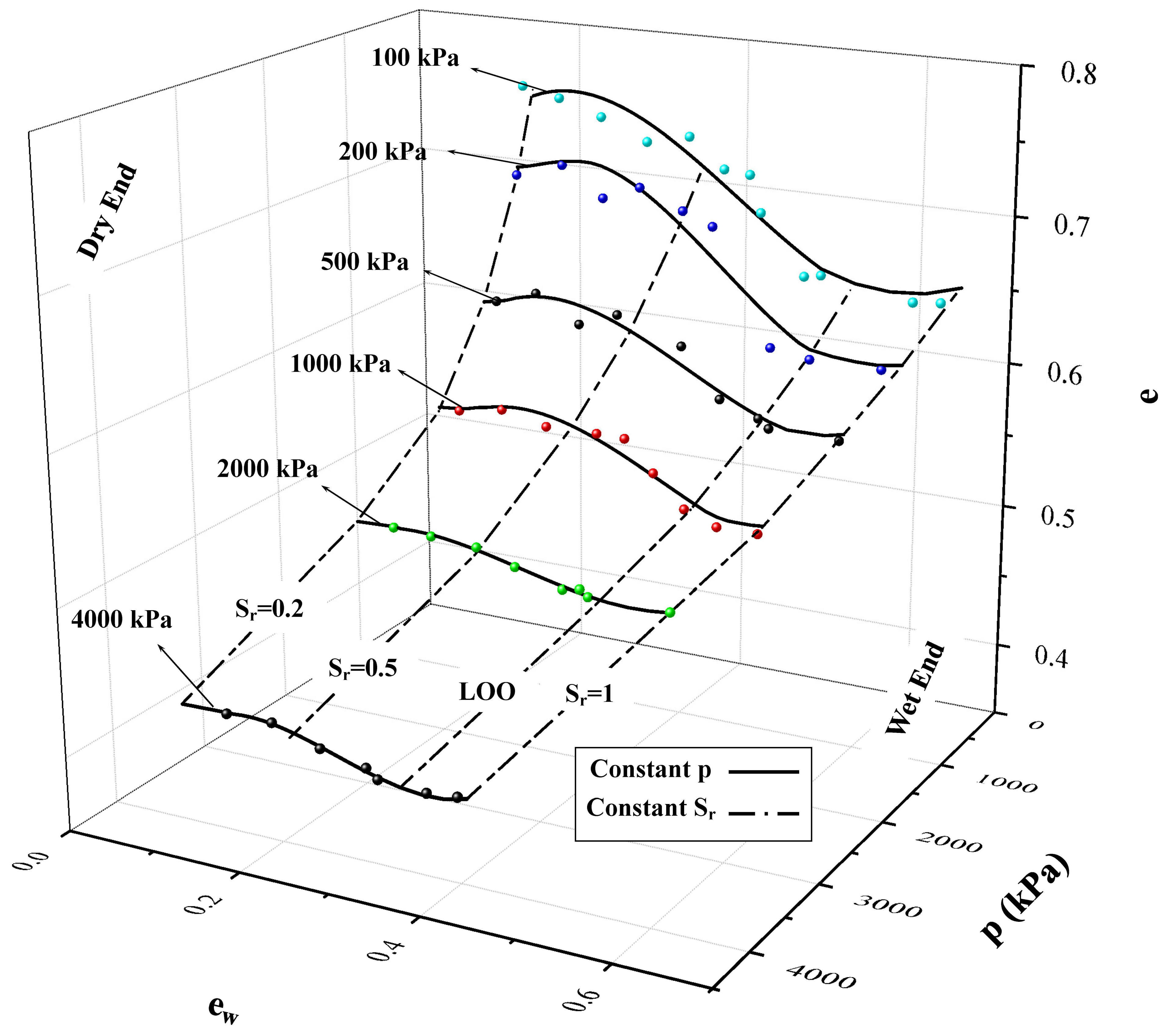

100 kPa
200 kPa
500 kPa
1000 kPa
2000 kPa
4000 kPa
Dry End
Wet End
S_r=0.2
S_r=0.5
LOO
S_r=1
Constant p
Constant S_r
0.8
0.7
0.6
0.5
0.4
e
0
1000
2000
3000
4000
p (kPa)
0.0
0.2
0.4
0.6
e_w

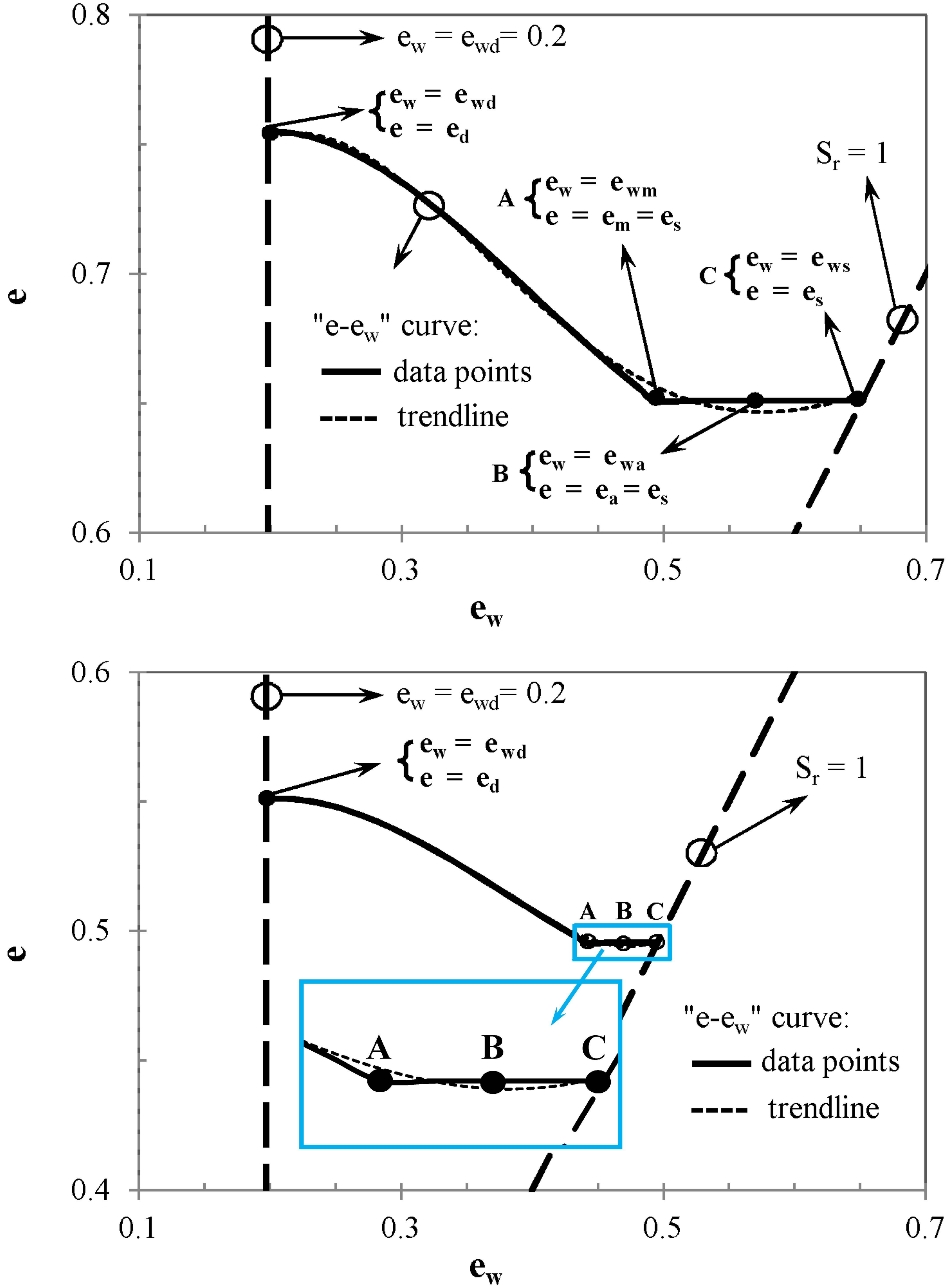

0.8
0.7
0.6
0.1
0.3
0.5
0.7
e
e_w
e_w = e_wd = 0.2
e_w = e_wd
e = e_d
A
e_w = e_wm
e = e_m = e_s
C
e_w = e_ws
e = e_s
S_r = 1
"e-e_w" curve:
data points
trendline
B
e_w = e_wa
e = e_a = e_s
0.6
0.5
0.4
0.1
0.3
0.5
0.7
e
e_w
e_w = e_wd = 0.2
e_w = e_wd
e = e_d
S_r = 1
A B C
A
B
C
"e-e_w" curve:
data points
trendline

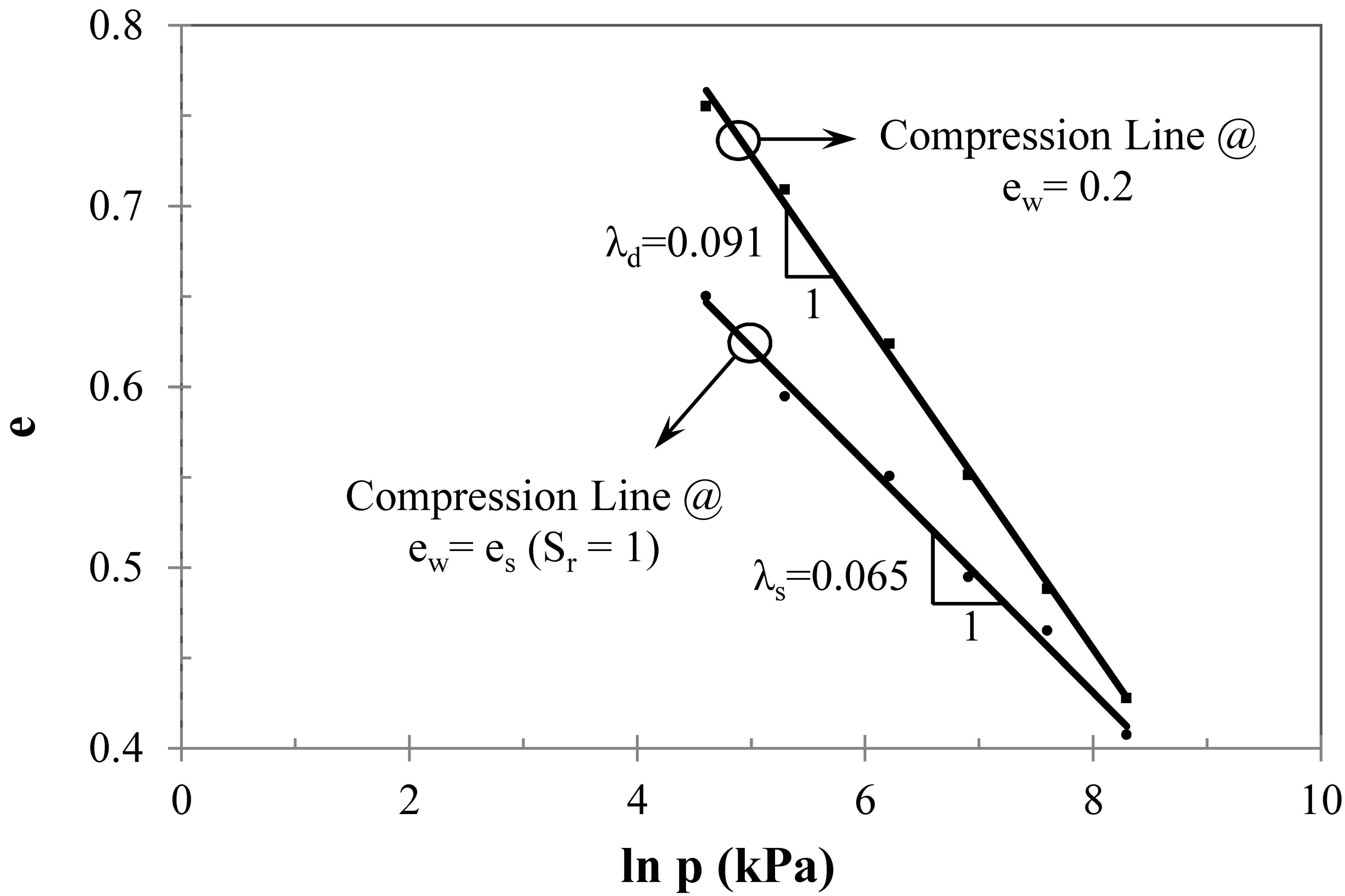
0.8
0.7
0.6
0.5
0.4
e
0
2
4
6
8
10
ln p (kPa)
Compression Line @
e_w= 0.2
λ_d=0.091
1
Compression Line @
e_w= e_s (S_r = 1)
λ_s=0.065
1

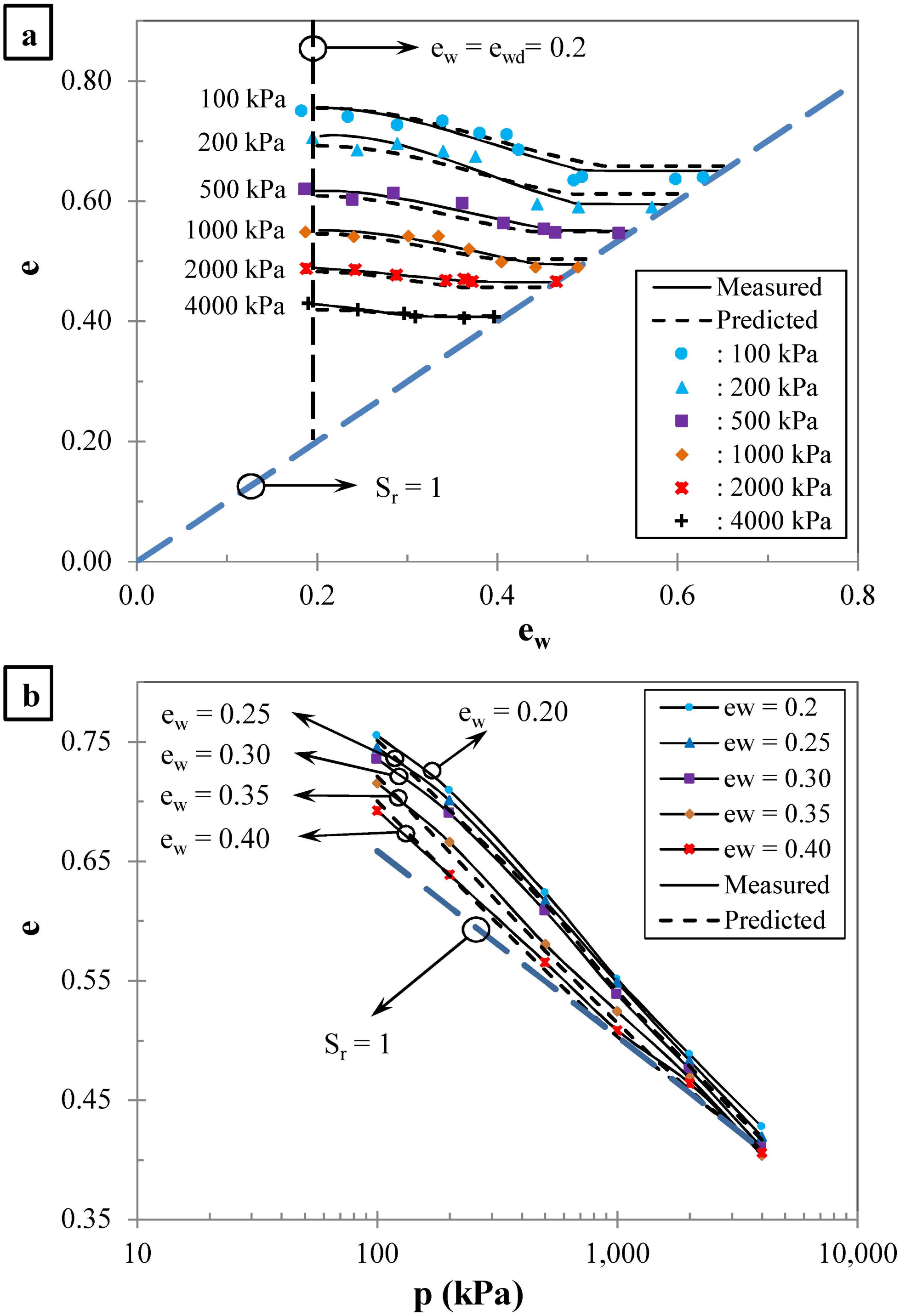

a
$e_w = e_{wd} = 0.2$
100 kPa
200 kPa
500 kPa
1000 kPa
2000 kPa
4000 kPa
$S_r = 1$
Measured
Predicted
: 100 kPa
: 200 kPa
: 500 kPa
: 1000 kPa
: 2000 kPa
: 4000 kPa
e
e_w
0.00
0.20
0.40
0.60
0.80
0.0
0.2
0.4
0.6
0.8
b
$e_w = 0.25$
$e_w = 0.30$
$e_w = 0.35$
$e_w = 0.40$
$e_w = 0.20$
$S_r = 1$
ew = 0.2
ew = 0.25
ew = 0.30
ew = 0.35
ew = 0.40
Measured
Predicted
e
p (kPa)
0.35
0.45
0.55
0.65
0.75
10
100
1,000
10,000

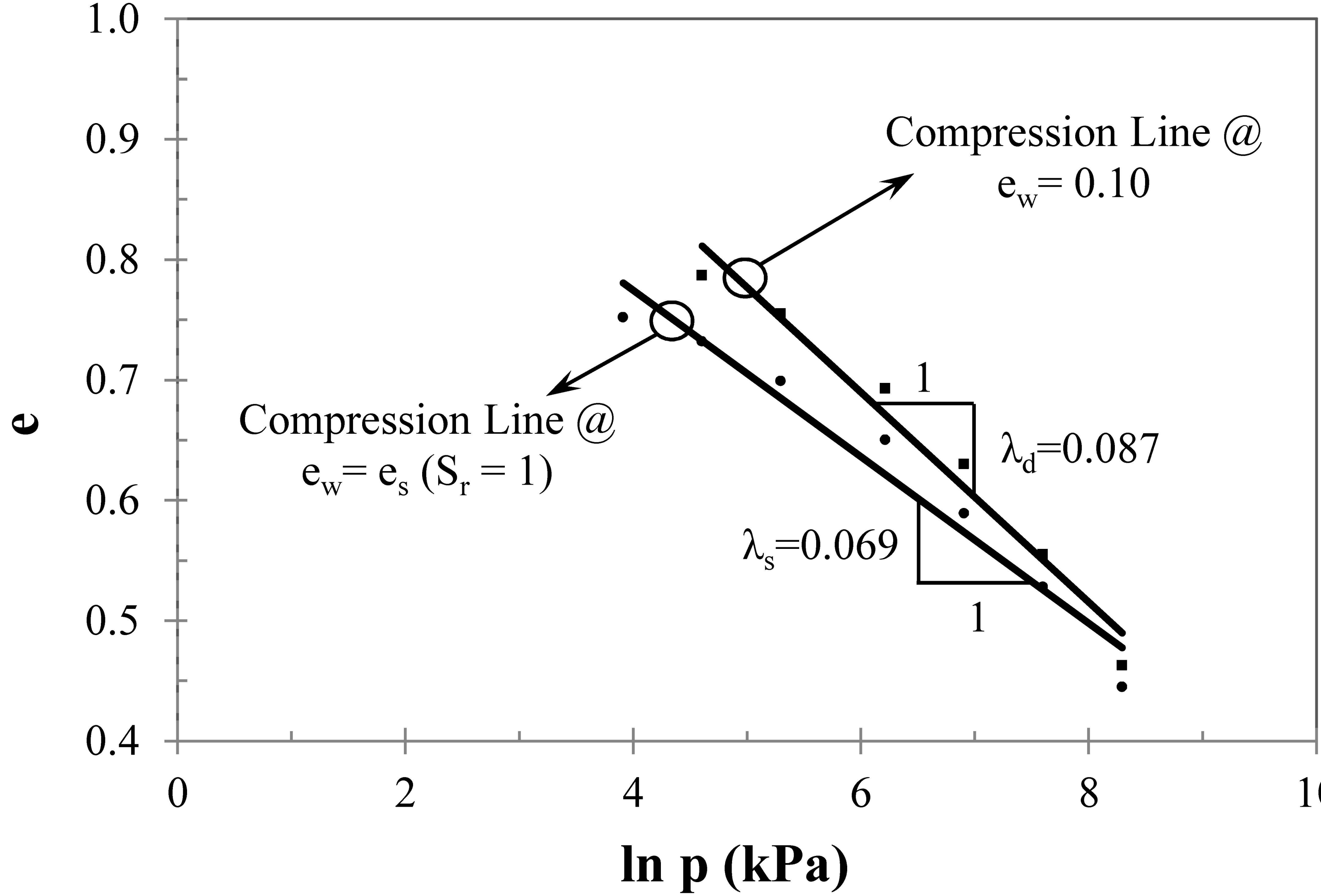

1.0
0.9
0.8
0.7
0.6
0.5
0.4
e
0
2
4
6
8
10
ln p (kPa)
Compression Line @
$e_w = 0.10$
Compression Line @
$e_w = e_s$ ($S_r = 1$)
1
$\lambda_d = 0.087$
$\lambda_s = 0.069$
1

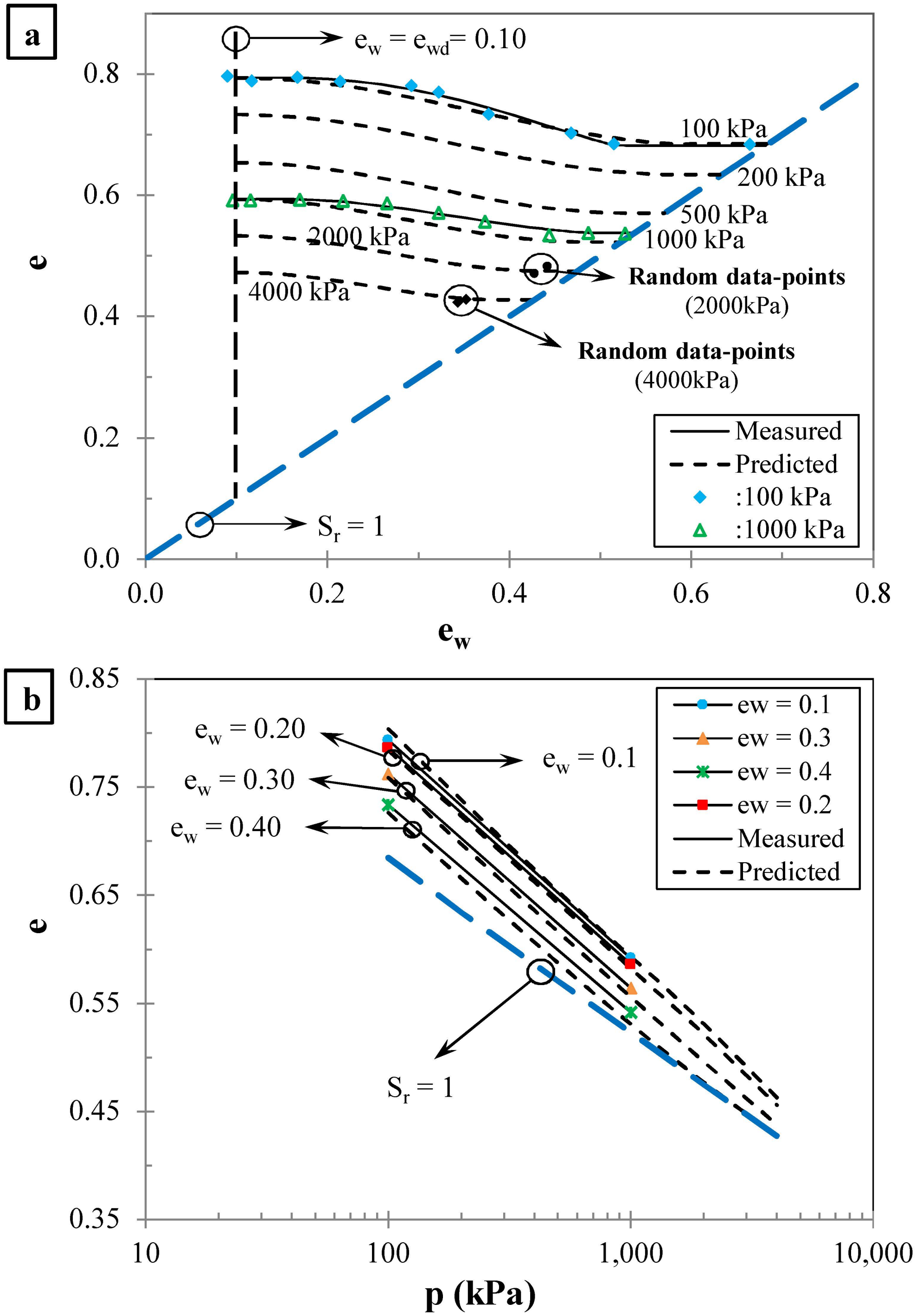
a
$e_w = e_{wd} = 0.10$
100 kPa
200 kPa
500 kPa
1000 kPa
2000 kPa
4000 kPa
Random data-points
(2000kPa)
Random data-points
(4000kPa)
$S_r = 1$
Measured
Predicted
:100 kPa
:1000 kPa
e
0.0
0.2
0.4
0.6
0.8
e_w
b
$e_w = 0.20$
$e_w = 0.30$
$e_w = 0.40$
$e_w = 0.1$
$S_r = 1$
ew = 0.1
ew = 0.3
ew = 0.4
ew = 0.2
Measured
Predicted
e
0.85
0.75
0.65
0.55
0.45
0.35
10
100
1,000
10,000
p (kPa)

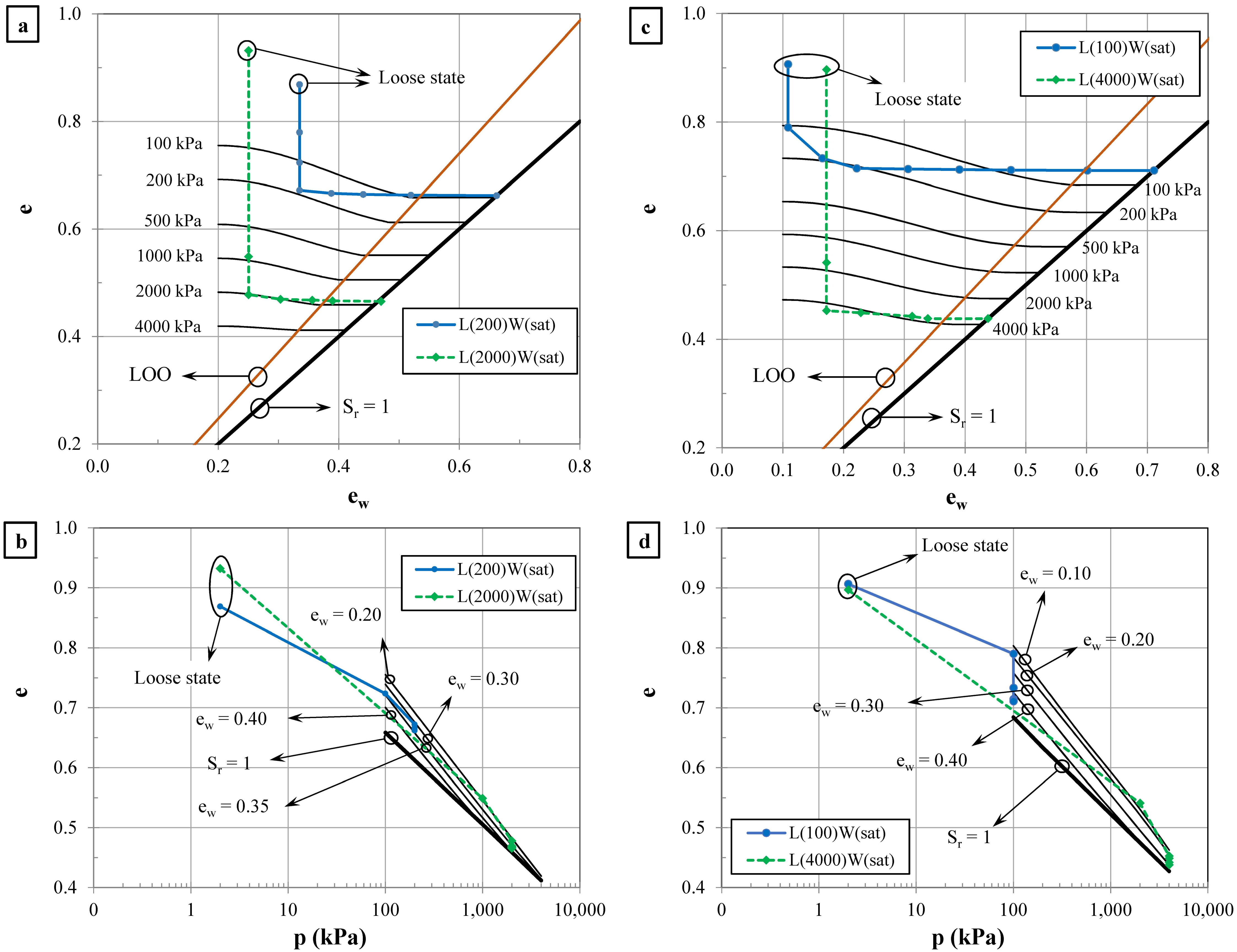
a
b
c
d
Loose state
LOO
$S_r = 1$
100 kPa
200 kPa
500 kPa
1000 kPa
2000 kPa
4000 kPa
L(200)W(sat)
L(2000)W(sat)
L(100)W(sat)
L(4000)W(sat)
$e_w = 0.10$
$e_w = 0.20$
$e_w = 0.30$
$e_w = 0.35$
$e_w = 0.40$
e
e_w
p (kPa)
0.0
0.1
0.2
0.3
0.4
0.5
0.6
0.7
0.8
0.9
1.0
0
1
10
100
1,000
10,000

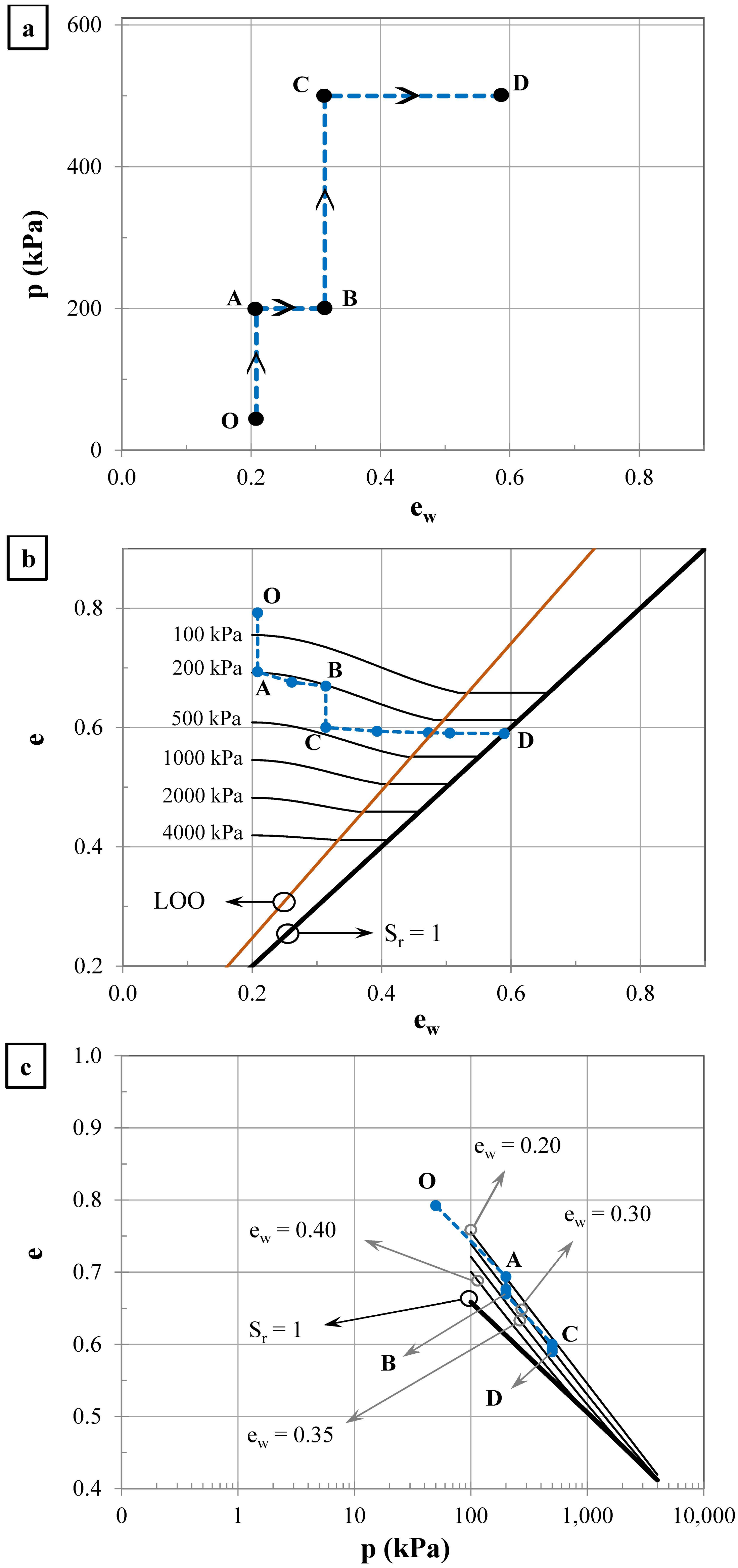
a
p (kPa)
e_w
O
A
B
C
D
b
e
e_w
100 kPa
200 kPa
500 kPa
1000 kPa
2000 kPa
4000 kPa
LOO
$S_r = 1$
c
e
p (kPa)
$e_w = 0.20$
$e_w = 0.30$
$e_w = 0.40$
$e_w = 0.35$
$S_r = 1$

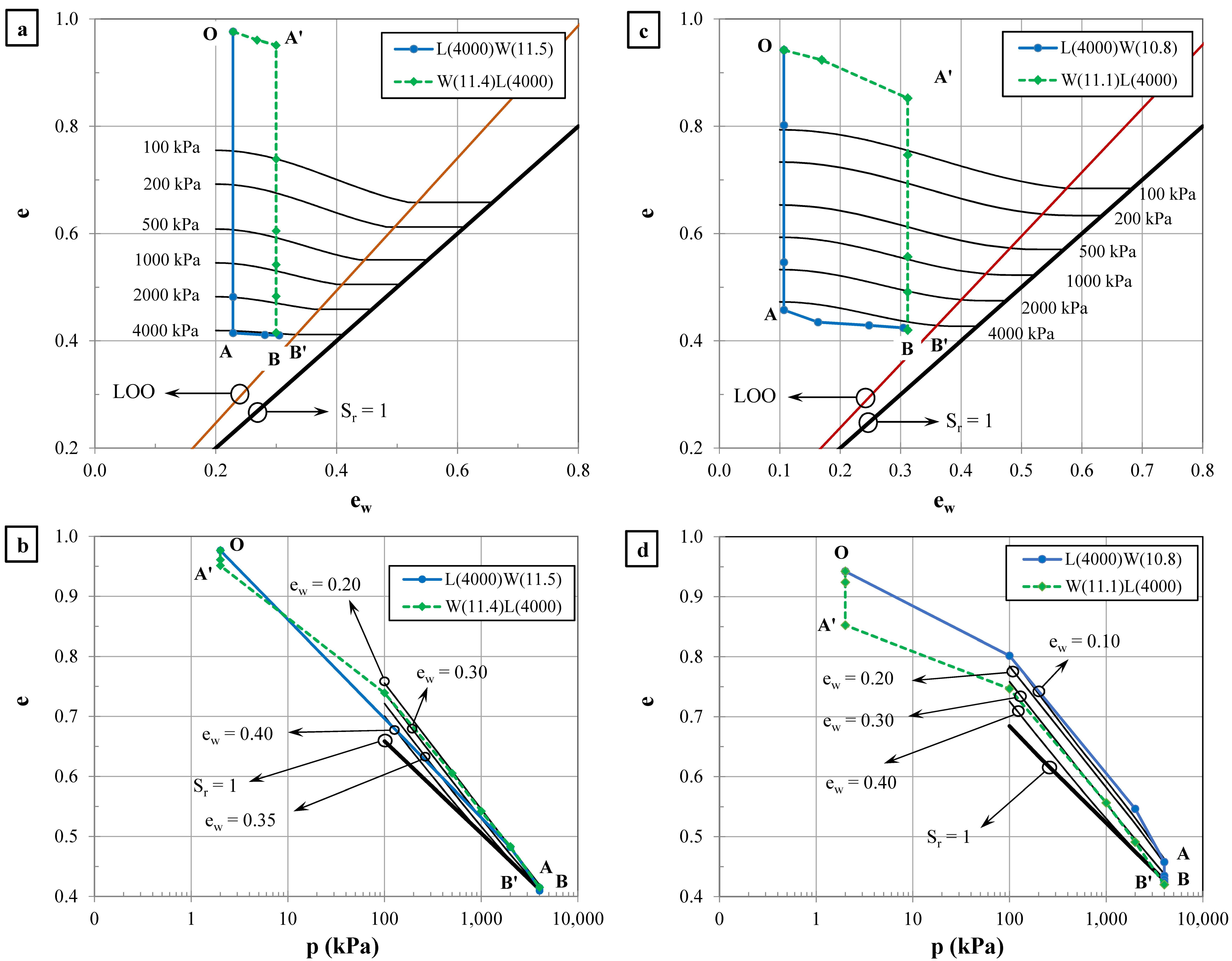

a
b
c
d
L(4000)W(11.5)
W(11.4)L(4000)
L(4000)W(10.8)
W(11.1)L(4000)
O
A
B
A'
B'
100 kPa
200 kPa
500 kPa
1000 kPa
2000 kPa
4000 kPa
LOO
$S_r = 1$
$e_w = 0.10$
$e_w = 0.20$
$e_w = 0.30$
$e_w = 0.35$
$e_w = 0.40$
e
e_w
p (kPa)